Cluster and THEMIS studies of Dayside Magnetospheric Boundary Layer Phenomena

Knut Stanley Jacobsen

May 12, 2010

Acknowledgments

Contents

Chapter 1

Introduction

The solar wind carries plasma and magnetic fields from the Sun. Being a gas of electrically charged particles, it will interact strongly with the magnetic field of the Earth. The main consequence of the interaction is that most of the solar wind is deflected around the Earth, but a detailed look reveals an abundance of complex processes which may, in extreme cases, affect our infrastructure by interfering with or destroying satellites and power grids. Fortunately, a more commonly observed effect is the generation of light in the upper parts of the atmosphere, known as Aurora. This thesis aims to increase our knowledge of the processes occurring in the boundary layers that connect the solar wind to the near-Earth environment. Of the three papers in this thesis, the first examines the consequences of a seemingly small change in the interplanetary magnetic field, which triggers a cascade of events that seriously disturb the magnetospheric boundary layers. This in turn leads to local disturbances of the magnetic field at the ground level. A large part of the field of space physics is the study of Magnetosphere–Ionosphere coupling (M-I coupling). Through waves, precipitating plasma and electrical currents, the forces applied to the magnetosphere by its interaction with the solar wind are transmitted down to the ionosphere. The second and third papers investigate interactions between the electric field, plasma and currents in the cusp, a region where solar wind plasma precipitates into the upper atmosphere.

The structure of this thesis is as follows. Sections 2 - 5 introduces concepts which are discussed in the papers, and sections 6 and 7 give short introductions to the Cluster and THEMIS missions, which were the main providers of data to these studies.
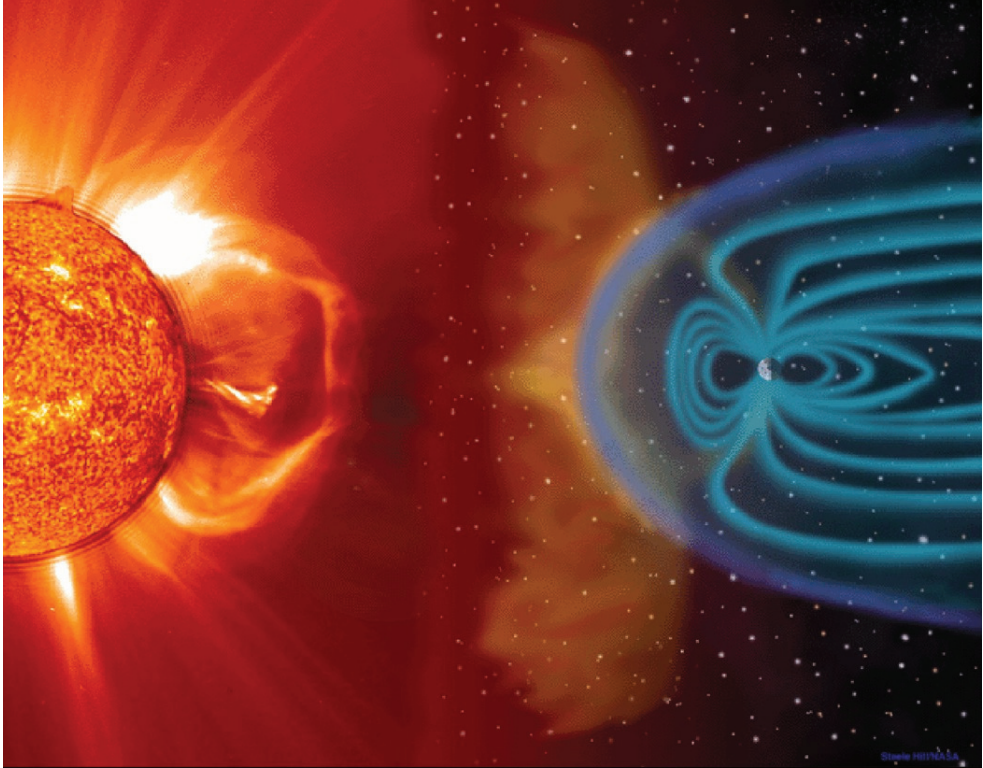
Figure 1.1: Illustration of the solar wind interacting with the Earth's magnetosphere. Not to scale. Credits: Magnetosphere: NASA, the Sun: ESA/NASA SOHO

Chapter 2

Dayside Magnetosphere boundary layers and related processes

Undisturbed by the solar wind, the magnetic field of the Earth is roughly equal to that of a dipole magnet, with field lines forming closed loops from the South to the North hemisphere. When disturbed by the solar wind it is compressed on the sunward side and extended on the antisunward side. The region in space that is dominated by the magnetic field of the Earth is called the magnetosphere. It is bounded by the magnetopause and surrounded by the magnetosheath, a region of heated and disturbed solar wind plasma. The boundary between the magnetosheath and the solar wind is called the bow shock.

The formation of the magnetosheath and bow shock is a result of the magnetic field of the Earth acting as an obstacle to the solar wind. As the solar wind flows at supersonic speeds, a shock is formed in front of the obstacle. The bow shock marks the boundary of plasma that has been disturbed by the presence of this obstacle. Solar wind plasma that passes the bow shock into the magnetosheath experiences several effects, with the main effect being a deflection around the magnetosphere (See Fig. 2.1). In addition to this, a part of its directed motion is converted into random motion (heat), and a small portion of the plasma is reflected.

When two magnetic fields meet they may, depending on the directionality of the magnetic fields, connect through the process known as reconnection. This frequently occurs when the solar wind magnetic field interacts with the magnetic field of the Earth at the magnetopause. After this reconfiguration, some magnetic field lines will have one end connected to the Earth and the other going out into the solar wind. These are referred to as open magnetic field lines, as plasma can access the atmosphere of the Earth along them. Field lines still in the modified dipole configuration, forming closed loops between the hemispheres, are referred to as closed field lines. The region of magnetic field lines that have recently connected to the magnetic field of the solar wind are referred to as the Cusp (See Fig. 2.2). The process of magnetic reconnection converts magnetic field energy to kinetic energy, releasing streams of energized plasma along the magnetic field lines. More energetic particles will travel faster, and thus the energy of the particles observed at some distance from the point of reconnection will depend on the time that has passed since the magnetic field line was involved in the process of reconnection.

One aspect of the M-I coupling is the flow of magnetic field aligned currents (FAC). These flow along the magnetic field lines into or out of the ionosphere, in which they can flow transverse to the magnetic field and connect to other field lines, eventually forming current loops. As
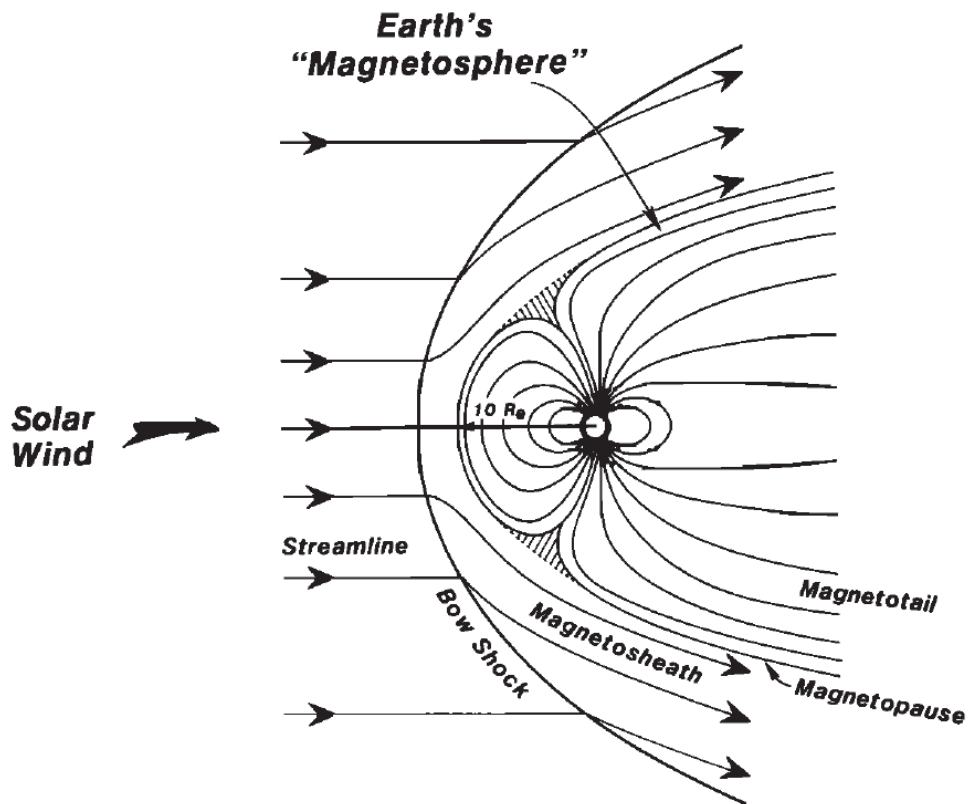
Figure 2.1: The major regions and boundaries formed due to the interaction between the solar wind and the magnetic field of the Earth. The motion of the solar wind plasma is indicated by streamlines. (Adapted from Luhmann and Brace (1991))
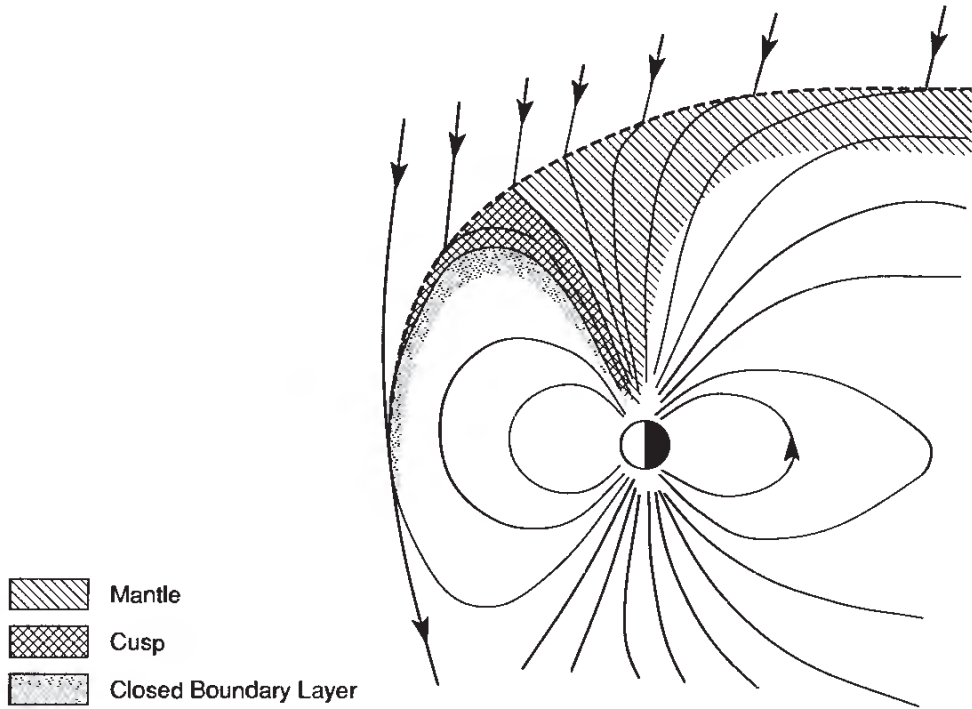
Figure 2.2: Figure 9.19 of Kivelson and Russell (1995). Regions in the vicinity of newly reconnected magnetic field lines. A plasma boundary layer may be found at closed field lines. The cusp consists of newly reconnected field lines, where plasma energized by the reconnection process precipitate into the atmosphere. The mantle consists of older field lines where there is no longer any precipitation of high energy plasma.
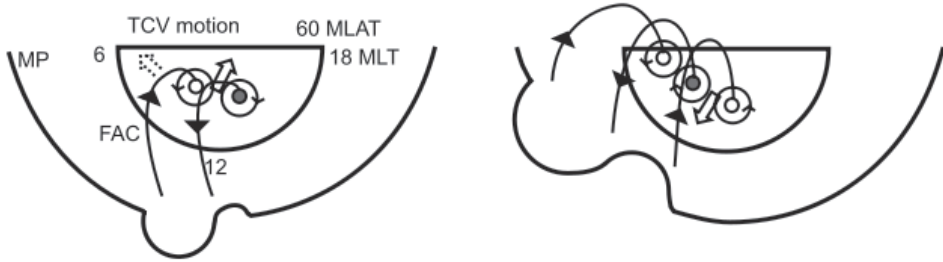
Figure 2.3: TCVs caused by tailward-moving magnetopause deformations. The left part shows how the magnetopause deformations connect via FACs to the ionosphere, where plasma convects around the FAC footpoints. The right part shows the situation at a later time, where the original vortices have moved towards the nightside as the deformations move tailward, and a new vortex has appeared as the deformations have grown in size. Adapted from Fig. 8 of Kataoka et al. (2002).

these currents flow through the ionosphere, they induce plasma flows and magnetic field disturbances. The large scale dayside current systems are discussed in section 3. Smaller, transient field-aligned currents may arise from e.g. transient magnetopause deformations. A propagating magnetopause deformation will create Travelling Convection Vortices (TCV), as described by Glassmeier (1992) and Kataoka et al. (2002). In a convection vortex, the plasma of the ionosphere flows in a circle around the footpoint of a FAC. If the location of the FAC moves, the vortex moves with it. The plasma forming the TCV does not have a bulk motion following the FAC footpoint. As the FAC footpoint moves, new plasma is set in motion, and the old plasma slows down as it is no longer affected by the forces caused by the currents. See Fig. 2.3.

Chapter 3

Current systems

Several large systems cause current to flow into or out of the ionosphere. This section is a short introduction to the large scale current systems present on the dayside part of the auroral oval.

These currents were first detected by the satellite 1963 38C (Zmuda et al., 1966), and Cummings and Dessler (1967) suggested a link to the current system proposed earlier by Birkeland (1908). Statistical studies by Iijima and Potemra (1976a,b) and Iijima et al. (1978) revealed the large-scale current pattern, which consisted of two rings of current, "Region 1" (R1) at higher latitudes and "Region 2" (R2) at lower latitudes. The direction of R2 current was downward in the dusk hemisphere and upward in the dawn hemisphere, and the direction of R1 current was the opposite of this. At higher latitudes a third system, the cusp currents, was associated with the dayside cusp (Iijima and Potemra, 1976b; Iijima et al., 1978; Wilhjelm et al., 1978; McDiarmid et al., 1978). The R2 and R1 currents are easily identified in recent statistical studies of FACs in the polar regions (e.g. Anderson et al. (2008), Green et al. (2009) and Juusola et al. (2009)). See also Fig. 3.1.

The R2 current is caused by the partial ring current (Cowley (2000) and references therein). The ring current flows in the trapped plasma at 3-5 Earth radii (R_E). Magnetic gradient drift causes ion to drift westward and electrons to drift eastward. If the plasma density was constant along the drift paths, the current would simply flow in a circle around the Earth. However, the ExB-drift caused by the dawn-to-dusk electric field shifts the plasma sunward, with the result that the number of electrons and ions drifting in opposite directions is not equal. For current continuity to be maintained FACs which can close the current through the ionosphere are required. A sketch illustrating this is shown in Fig. 3.2.

The R1 currents are commonly thought to flow on the outer surface of the plasma sheet up to the magnetopause currents, which drive the system (e.g. Cowley (2000) and references therein). However, Stern (1983) suggested that near noon they may flow on open field lines, and there have been observations of R1 currents partially on open field lines (Beaujardiere et al., 1993; Xu and Kivelson, 1994; Lopez et al., 2008). It has been proposed that when the polar cap potential is saturated, the R1 current replaces the Chapman-Ferraro current as the primary force balance versus the solar wind pressure (Siscoe et al., 2002a,b). This requires a part or all of the R1 current to flow on open field lines (Siscoe, 2006).

The nature of the cusp currents is discussed by Taguchi et al. (1993), who referred to them as the low-latitude cleft current (LCC) and the high-latitude cleft current (HCC). They appear as pairs of latitudinal bands of FAC around noon, with FACs in opposite directions (See Fig.
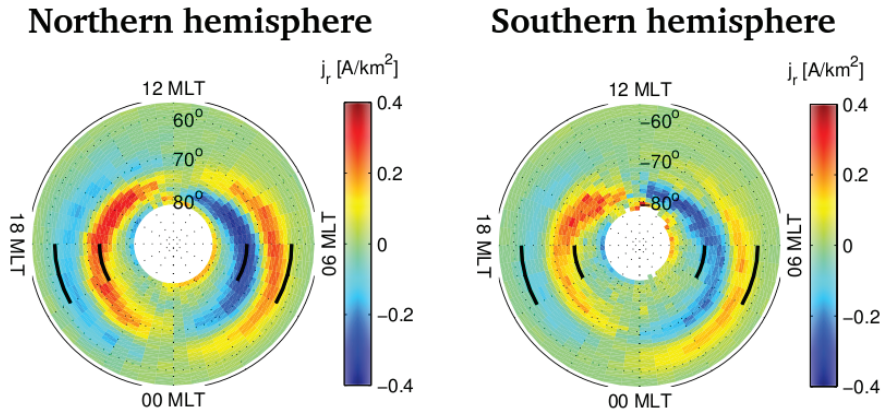
Figure 3.1: Statistical FAC density in the northern and southern hemispheres. The innermost bands are the R1 currents, the outermost bands are the R2 currents. Note that the color coding used here is opposite to the color coding used in paper 3 (red and blue are switched). Adapted from Fig. 3 of Juusola et al. (2009).
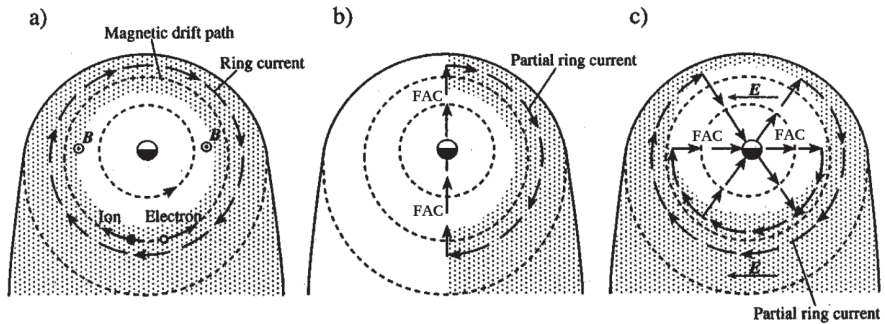
Figure 3.2: Sketches of the equatorial magnetosphere showing the FAC flow which connects the magnetospheric and ionospheric current systems (long-dashed lines) required by current continuity, for various spatial distributions of hot ring current plasma (dotted regions). The short-dashed lines represent the magnetic drift paths of ions and electrons, with ions drifting to the west and electrons to the east. In sketch a, the plasma is distributed uniformly around the drift paths, such that the drift current is divergence-free in the magnetosphere and no FAC flows. In sketch b, the initial plasma distribution has higher densities at dawn than at dusk, such that the partial ring current at dawn must close in the ionosphere via downward FACs at midnight and upwards FACs at noon. Sketch c shows the situation produced from an initial equilibrium by an interval of sunward flow imposed by a dawn-to-dusk electric field E. A partial ring current is formed centred on midnight, which closes via downward FAC at dusk and upward FAC at dawn. (Figure and caption from Cowley (2000))

By ≥ 5 nT   By ≤ - 5 nT

(a)   (b)

LCC   LCC
HCC   HCC

REGION OF   REGION OF
UPWARD   DOWNWARD
FIELD-ALIGNED CURRENT   FIELD-ALIGNED CURRENT
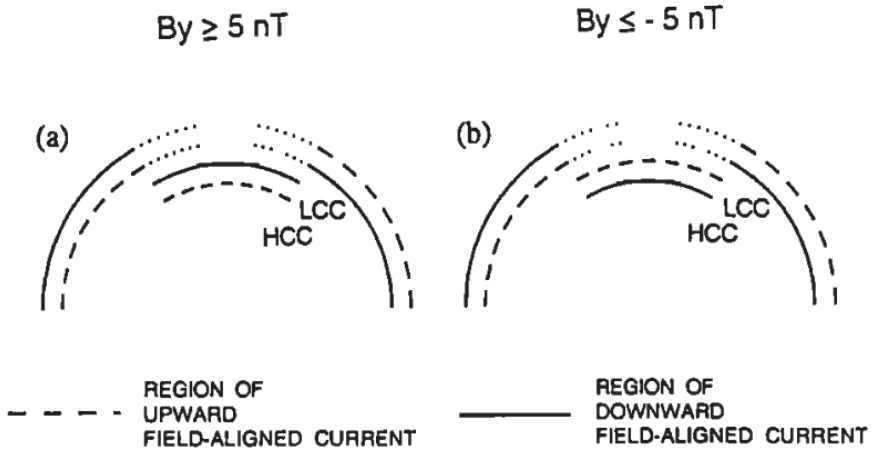
Figure 3.3: Figure 7 of Taguchi et al. (1993). The schematic model of Taguchi et al. of the near-noon currents poleward of the R2/R1 currents.

3.3). In the north hemisphere, the most equatorward FAC band will be downward/upward for IMF B_Y positive/negative and lies on the equatorward edge of the cusp. The direction of the currents is opposite for the south hemisphere. They are caused by the open magnetic field lines connecting the electric field immediately inside the magnetopause to the ionosphere (See Fig. 3.4).

(a)

J_{source}

LCC HCC

B'

A'

B

A

$V_{RC} + V_{SH}$

V_{SH}

V_{RC}

V_{RC}

$V_{RC} + V_{SII}$

V_{SII}

(b)

6   b   IONOSPHERE   18

a

12

DOWNWARD FAC

UPWARD FAC
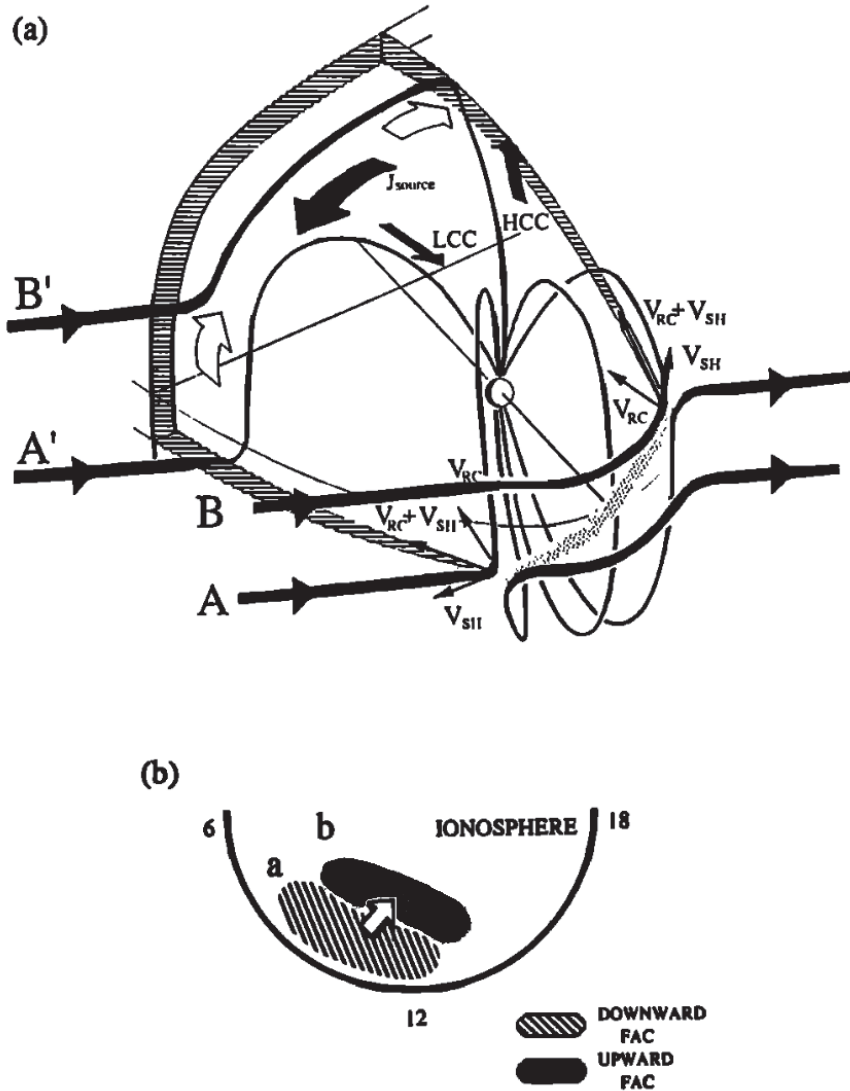
Figure 3.4: Figure 8 of Taguchi et al. (1993). Schematic view of the current-generating mechanism behind the currents shown in Fig. 3.3.

Part **a**: The IMF (field lines A and B) connects to the magnetic field of the Earth in the dotted region. Field lines are then pulled by magnetic tension (V_{RC}) and carried downstream by the magnetosheath plasma (V_{SH}). At a later time, the field lines have moved to the positions A' and B', where they connect the electric field (open arrows) and currents (big black arrow) just inside the magnetopause to the ionosphere. The region just inside the magnetopause thus acts as a generator driving current into and out of the ionosphere through the low- and high-latitude cleft currents (black arrows labeled LCC and HCC).

Part **b**: Resulting regions of FAC and a projected electric field (open arrow) in the ionosphere. A more detailed discussion can be found in Taguchi et al. (1993).

Chapter 4

Electric fields in the cusp

4.1 Low frequency fluctuations

In the cusp, energy and plasma from the magnetosheath, energized by reconnection, flows down towards the ionosphere. On the way down, the waves and particles interact with themselves and each other, generating new waves in a large range of frequencies. These intense low-frequency fluctuations of the electric field have been observed at altitudes ranging from the ionosphere up to 10 R_E (e.g. Gurnett and Frank (1977); Maynard et al. (1982); Sugiura et al. (1982); Gurnett et al. (1984); Marklund et al. (1990); Matsuoka et al. (1991, 1993); Kintner et al. (1996); Stasiewicz et al. (2000); Ivchenko and Marklund (2001); Grison et al. (2005)), and is commonly referred to as broadband extremely low frequency (BB-ELF) electric fields (e.g. Wahlund et al. (1998); Knudsen et al. (1998); Kintner et al. (2000); Lund et al. (2000); Lynch et al. (2002); Hamrin et al. (2002); Bogdanova et al. (2004); Burchill et al. (2004); Backrud et al. (2005); Tam et al. (2005)). The term BB-ELF has been used to refer to different frequency ranges by different authors, but generally it covers a frequency range from below the ion cyclotron frequency to above the ion plasma frequency. The BB-ELF phenomenon has been connected to the auroral oval, in particular the cusp, (e.g. Miyake et al. (2003); Kasahara et al. (2001)) and to ion heating (e.g. Wahlund et al. (1998); Knudsen et al. (1998)). It has been shown that BB-ELF waves may be a part of the ion heating mechanism that leads to ionospheric ion outflow (Bouhram et al., 2002), energizing ions in the upper atmosphere to the point that they flow out into the magnetosphere. Matsuoka et al. (1993) quantified the relationship between the BB-ELF activity and precipitating particle fluxes using data from EXOS D. This issue is revisited and expanded upon in the second paper of this thesis, using new data from the Cluster mission.

4.2 Quasi-static electric field structures

Quasistatic magnetic-field-aligned electric fields is the main mechanism for acceleration of auroral particles. They are found at altitudes below 3-3.5 R_E (Mozer and Hull, 2001). The acceleration region has been studied, for example, by the S3-3, DE-1, Viking, Akebono, Freja, FAST, Polar, DMSP and Cluster satellites (e.g. Lundin and Eliasson (1991); McFadden et al. (1999); Mozer and Hull (2001); Olsson and Janhunen (2003); Hamrin et al. (2006); Maggiolo et al. (2006); Borg et al. (2007)). Above 3.5 R_E, there are no significant field-aligned electric

fields, but strong bipolar or monopolar electric fields are observed perpendicular to the magnetic field. The low and high altitude electric fields are connected by a U- or S-shaped potential structure (Carlqvist and Bostrom, 1970; Mozer et al., 1980) (See Fig. 4.1). The signature in a energy-time spectrogram of precipitating electrons accelerated by a field-aligned electric field is referred to as an 'inverted V' (See Fig. 4.2). These are frequently observed both in the nightside and dayside parts of the auroral oval (Lin and Hoffman, 1982). The dayside inverted Vs are smaller and less energetic than those at the nightside (Lin and Hoffman, 1982). Upward-pointing field-aligned electric fields accelerate electrons downwards. When these energetic electrons encounter the atmosphere, they transfer energy to atoms through collisions. This energy is subsequently released as light, creating the aurora (See Fig. 4.3). Downward-pointing field-aligned electric fields, on the other hand, accelerates electrons upward. This may prevent precipitating electrons from reaching the atmosphere, resulting in bands in the aurora where there is no light emitted, known as 'black aurora' (See Fig. 4.4).

As to the cause of these electric fields, it has been suggested that they are formed in response to a current imposed by a large-scale current system. The simplest way to understand this is to consider the equation for current:

$$j = q_e n_e v_e + q_i n_i v_i$$

where j is current, q is the charge of a particle, n is the particle density and v is the particle velocity, with subscripts e/i for electrons/ions, respectively. Generally, $|q_e| = |q_i|$, $n_e = n_i$ and $v_e \gg v_i$, which means that the electrons are the current carriers. The charge of an electron is a constant, and the density is given by the source region. Thus if the value of the current j, imposed by outside conditions, exceeds the product $q_e n_e v_e$, the electron velocity is the parameter that must be increased. This can be achieved by a field-aligned electric field. For detailed discussions on the mechanisms through which these fields are created and maintained, see for example Knight (1973) and Lyons (1980).

The study of quasi-static electric field structures in the dayside cusp region is the subject of the third paper of this thesis.
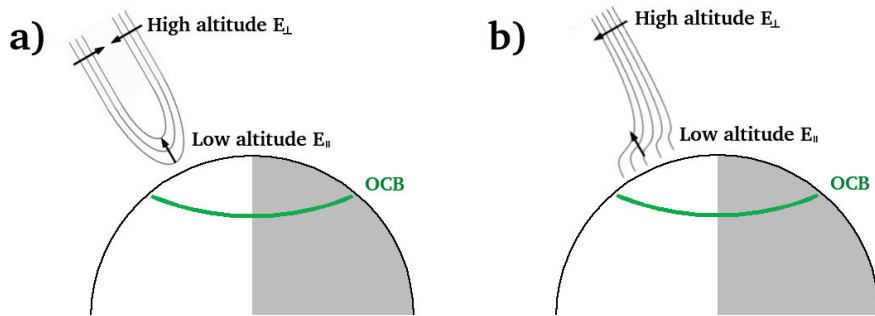
Figure 4.1: Illustration of the electric potential structures linking high-altitude and low-altitude electric fields. Not to scale. Panel **a** shows a U-shaped potential structure, while panel **b** shows an S-shaped potential structure. The green line marks the open-closed magnetic field line boundary (OCB). Note that the electric fields may also point in the opposite directions of what is shown here.
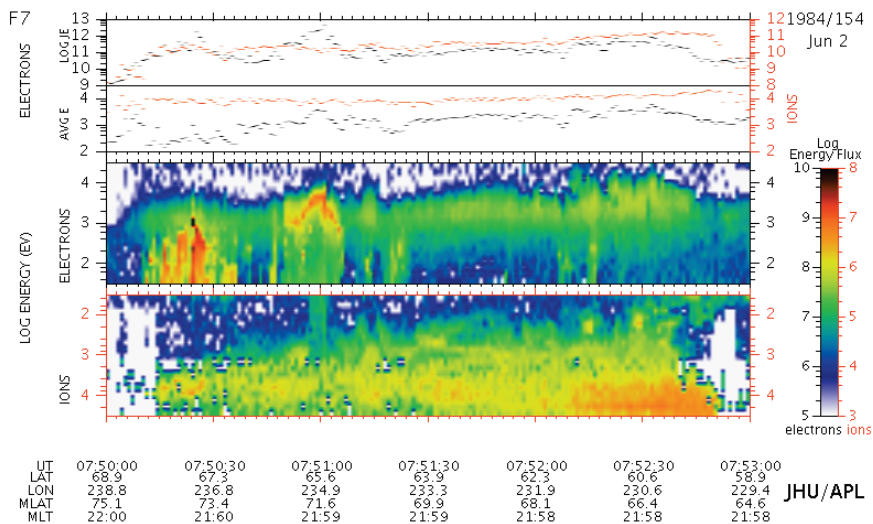
Figure 4.2: Data from a low-altitude satellite (DMSP F7). In the electron spectrogram (third panel), a textbook example of an inverted V signature is seen at $\sim$ 7:51. Plotted using JHU/APL plotting tool.

Figure 4.3: Aurora seen from space. Credit: NASA
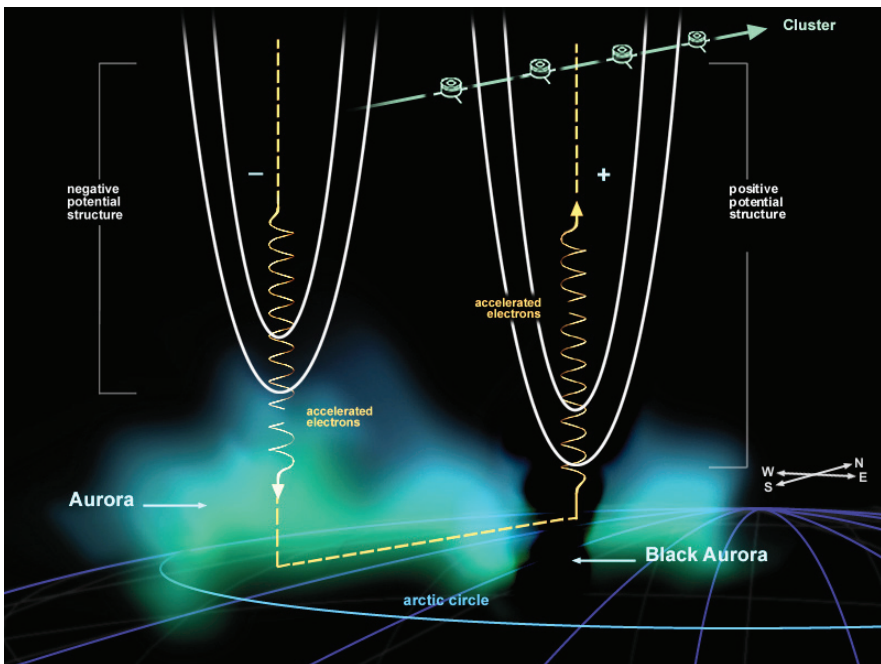
Figure 4.4: On the left, a U-shaped electric potential structure with a upward-pointing field-aligned electric field. A satellite passing under this structure would observe an inverted V. On the right, a U-shaped electric potential structure with a downward-pointing field-aligned electric field. This prevents the flow of precipitating electrons, and thus there is no aurora underneath. Credit: ESA 2001. Illustration by Medialab

Chapter 5

Hot Flow Anomalies

Hot Flow Anomalies (HFA) were first discovered in the mid 1980s, in association with the passage of interplanetary current sheets (Schwartz and et al., 1985; Thomsen et al., 1986). Their main characteristic is a region of hot, tenuous plasma with a decreased magnetic field magnitude, moving in a direction different from the solar wind flow. They are observed in the solar wind close to the bow shock. A number of simulations were performed, exploring different theoretical explanations for the phenomenon. Burgess and Schwartz (1988) found that a magnetic field reversal (a tangential discontinuity in the magnetic field) convecting into a shock led to over-reflection followed by upstream penetration of ions from the shock. The reflected ions are thermalized through ion beam instabilities, causing a large increase in plasma temperature and pressure. Due to the increased pressure, the plasma expands, causing the density and the magnetic field strength to drop. At the boundary of the expanding HFA region, the plasma and the magnetic field may be compressed. Burgess (1989) investigated the role of the convection electric field ($-\mathsf{V} \times \mathsf{B}$) and found that a convection electric field pointing towards the discontinuity is necessary to focus the reflected ions into the discontinuity (See Fig. 5.1). Thomsen et al. (1993) provided an observational test of the importance of the convection electric field, which confirmed the results of the simulations by Burgess.

Interest in HFAs was renewed in the late 1990s, as observations were made of a large magnetopause deformation associated with a HFA. (Sibeck et al., 1998, 1999) They found an outward movement of 5 R_E in 7 minutes resulting from a HFA. Strong HFAs cause density variations not only in the upstream solar wind, but also in the downstream magnetosheath. As these reach the magnetopause the varying pressure cause magnetopause deformations. This causes FACs, which in turn create TCVs in the ionosphere. Schwartz et al. (2000) performed a study of 30 HFAs, and amongst other results, calculated an occurrence rate of 3 per day. These results indicated that HFAs are more common and have a far greater influence on the magnetosphere than previously thought. Sibeck et al. (2000) further investigated HFAs, and a short summary of their conceptual HFA model can be seen in Fig. 5.2. Examples of recent work on HFAs can be found in Lin (2002), Facsko et al. (2008), Eastwood et al. (2008) and Masters et al. (2009). The relative importance of strong HFAs on magnetospheric processes has still not been fully explored. The first paper of this thesis is a case study of a very strong HFA, using data from multiple satellites and ground observatories to explore the entire chain of events.
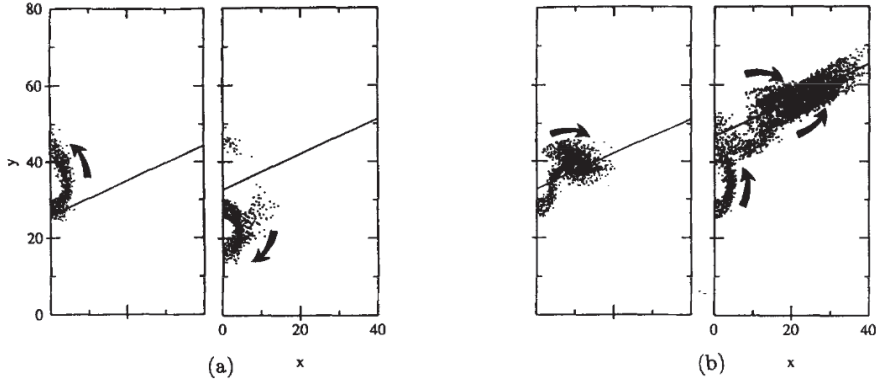
Figure 5.1: Simulation of particle movement in the vicinity of a magnetic field tangential discontinuity (TD). For **a**, the convection electric field points away from the TD, and the particles are displaced away from the TD. For **b**, the convection electric field points towards the TD, and the particles drift towards, and subsequently move along, the TD. (Adapted from Burgess (1989))
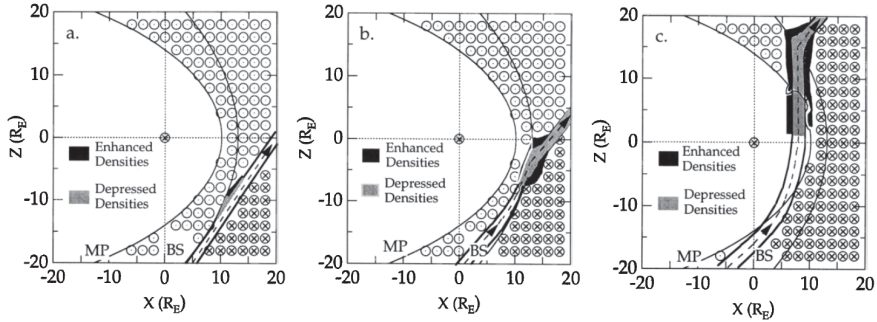
Figure 5.2: The interaction of a slab of sunward and northward IMF lines with the bow shock and magnetopause. Prior to the arrival of the slab, the IMF points dawnward. After the arrival of the slab, the IMF points duskward. (a) The slab's first encounter with the southern bow shock is shown. The region to which reflected ions gain access, thermalize, and depress IMF densities and magnetic field strengths to form a cavity upstream from the bow shock (shown in light shading) is rather limited. As the cavity expands, it compresses the surrounding solar wind plasma, enhancing densities and magnetic field strengths (shown in dark shading). (b) The situation when the intersection of the IMF slab with the bow shock has moved northward and parts of the cavity have been transmitted through the southern bow shock is shown. A region of enhanced densities and magnetic field strengths has formed on the trailing edge of the slab. (c) The situation at a later time when the density variations associated with the slab alternately compress the magnetopause and allow it to expand outward is shown. (Figure and caption from Sibeck et al. (2000))

16

Chapter 6

Cluster

Cluster (Credland et al., 1997; Credland and Schmidt, 1997) is a constellation of four spacecraft orbiting the Earth in a tetrahedron formation (See Fig. 6.1). The orbit is polar and elliptical, and during a year the point of apogee rotates from the magnetotail, through the flanks of the magnetosphere, out into the subsolar solar wind, and back to the magnetotail (See Fig. 6.2). Because of this, mid-altitude (4-6 R_E) cusp passes occur only during the autumn months (mainly September and October). During the years 2001 to 2005, the distance between the spacecraft has been varied in a range between 100 and 10000 kilometres, in order to measure phenomena at different scales.

The Cluster spacecraft are equipped with identical instrumentation. Of the 11 instruments, the following have been used in this thesis:

- The Cluster ion spectrometry instrument (CIS) (Reme et al., 1997) measures full 3D ion distributions over an energy range of ∼0-40 keV with a maximum resolution of one spin period, which is 4 seconds. The CIS instrument on Cluster 2 does not work.

- The plasma electron and current experiment (PEACE) (Johnstone et al., 1997) measures full 3D electron distributions over an energy range of 0.7 eV to 30 keV with a maximum resolution of half a spin period.

- The fluxgate magnetometer (FGM) (Balogh et al., 1997) measures the magnetic field at 22 Hz, or 67 Hz when in burst mode.

- The electric field and wave experiment (EFW) (Gustafsson et al., 1997) measures DC and low frequency electric fields at 25 Hz, or 450 Hz when in burst mode.

- The research with adaptive particle imaging detectors instrument (RAPID) (Wilken et al., 1997) measures high-energy ions and electrons with a maximum resolution of one spin period. It has an energy range of 30-1500 keV for ions and 20-450 keV for electrons.
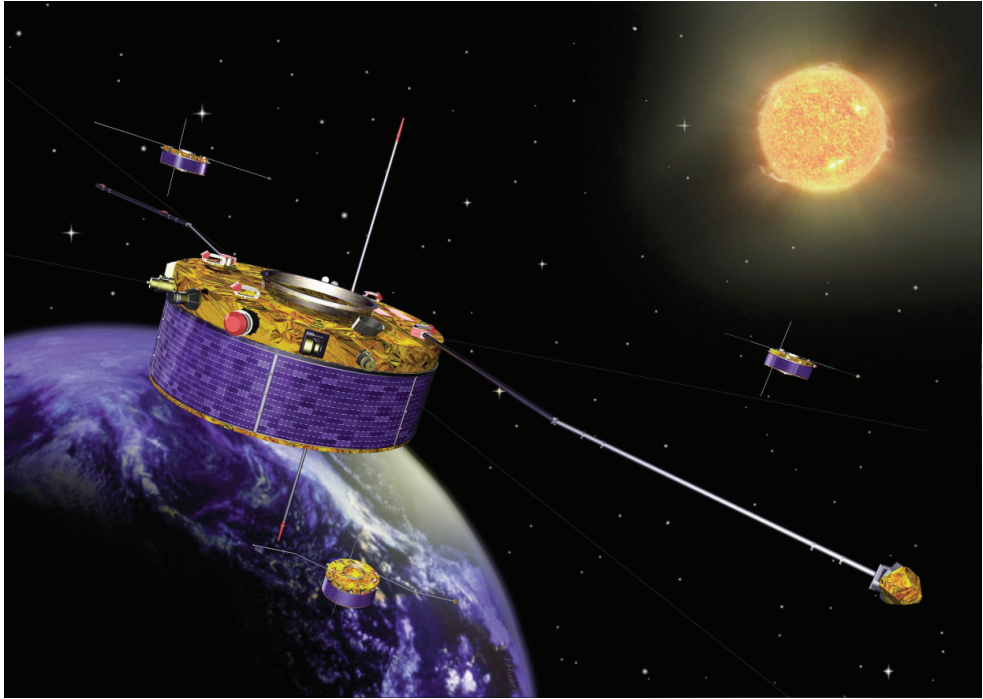
Figure 6.1: Artistic rendering of the Cluster spacecraft. Credit: ESA
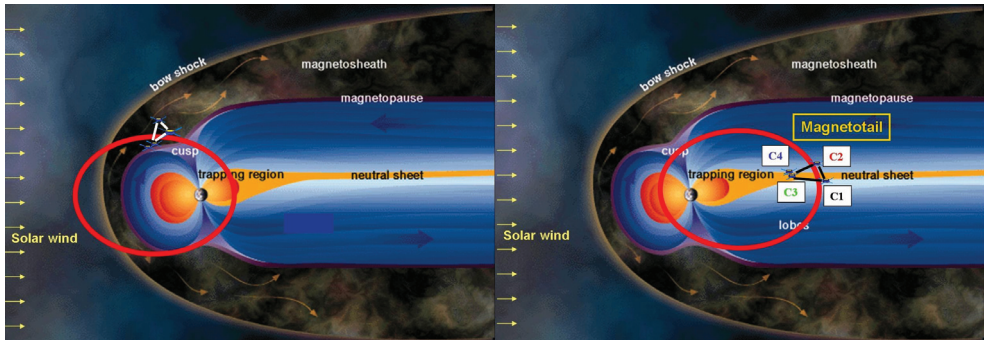
Figure 6.2: The left part shows the spring orbit of the Cluster spacecraft, while the right part shows the autumn orbit. Credit: ESA

Chapter 7

THEMIS

The Time History of Events and Macroscale Interactions during Substorms mission (THEMIS) (Angelopoulos, 2008) employs five spacecraft (See Fig. 7.1) and numerous ground-based instruments (Russell et al., 2008; Mende et al., 2008), with a primary objective of investigating substorms. In this thesis, data from THEMIS has been used to address one of its secondary objectives, dayside interactions. Following initial adjustments of the orbit, the THEMIS spacecraft have followed elliptical trajectories in the equatorial plane. Their orbits are designed to have them line up radially when they are at apogee, with three spacecraft close together at 10-12 R_E and the other two at 20 and 30 R_E. The apogees slowly rotate around the Earth, covering various areas of the magnetosphere as well as the dayside boundary layers (See Fig. 7.2).

The THEMIS spacecraft are equipped with identical instrumentation. Of the 5 instruments, the following have been used in this thesis:

- The THEMIS ion and electron electrostatic analyzers (iESA and eESA) (McFadden et al., 2008) measure plasma over the energy range from a few eV up to 30 keV for electrons and 25 keV for ions with a maximum resolution of one spin period, which is 3 seconds.

- The THEMIS Flux Gate Magnetometer (FGM) (Auster et al., 2008) measures the background magnetic field and its low frequency fluctuations with a resolution of up to 64 Hz.

Figure 7.1: Artists concept of the THEMIS spacecraft in orbit. Credit: NASA
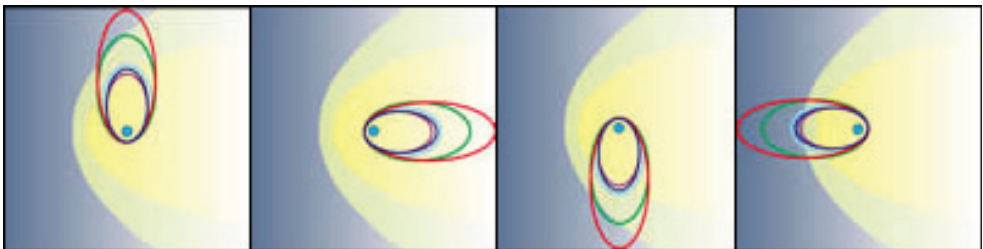
Figure 7.2: The 5 THEMIS spacecraft follow different elliptical orbits. During a year the orbits rotate around the Earth, covering different regions. Credit: UCB/SSL

Chapter 8

Summary of the papers

Paper #1: THEMIS observations of extreme magnetopause motion caused by a hot flow anomaly

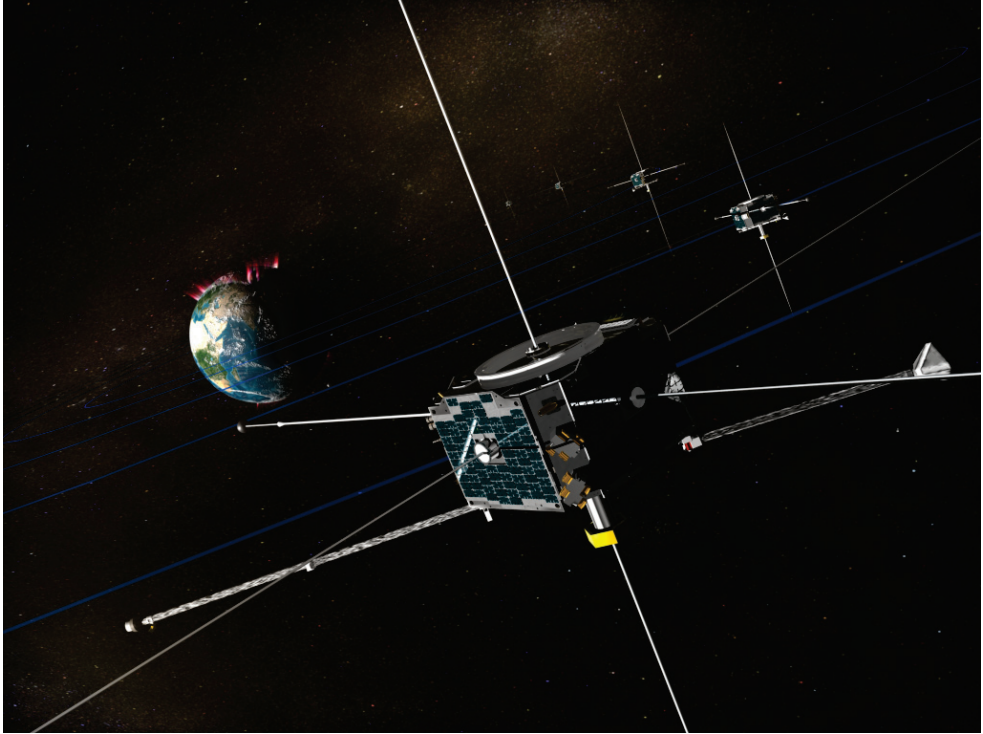K. S. Jacobsen, T. D. Phan, J. P. Eastwood, D. G. Sibeck, J. I. Moen, V. Angelopoulos, J. P. McFadden, M. J. Engebretson, G. Provan, D. Larson, and K.-H. Fornacon

The first paper is a case study of the interaction of a magnetic discontinuity in the interplanetary magnetic field with the bow shock. This resulted in a HFA which caused part of the magnetosphere to move outwards more than 5 R_E in just a minute. Judging from the magnetopause displacement, this event appears to be the strongest HFA on record. Combining data from the THEMIS spacecraft with data from the Advanced Composition Explorer spacecraft (ACE) (Stone et al., 1998), ground radars and ground magnetometers, the entire chain of events from the distant solar wind to the ground has been examined. While ACE provided data on the undisturbed solar wind, THEMIS B was located just a few R_E outside the bow shock and could measure the disturbances caused by the HFA. THEMIS C was located in the magnetosheath at the time, and the last three THEMIS spacecraft were spread out inside the magnetosphere, close to the magnetopause. As the magnetopause moved in response to the density variations in the magnetosheath, it passed twice over each of these four spacecraft. Through MVA analysis we found the local orientation of the magnetopause for each crossing, and when combined with an analysis of the timing of the encounters this allowed a reconstruction of the shape of the deformed magnetopause. On the ground, the SuperDARN radars observed convection vortices. However, the time resolution of SuperDARN was insufficient to track their movements. Using ground magnetometers, we first observed convection vortices passing a station very close to the path they were expected to follow based on the SuperDARN images. Then, using a chain of magnetometers across the US and Canada, we could observe the subsequent movement of the vortices.

Paper #2: On the correlation between Broad-Band ELF wave power and ion fluxes in the cusp

K. S. Jacobsen and J. I. Moen

The second paper investigates an aspect of the local particle-wave interactions in the cusp. A commonly occurring feature in the precipitation regions near the open-closed field line boundary (OCB) is intense low-frequency fluctuations of the electric field, referred to as broad-band extremely low frequency (BB-ELF) electric field fluctuations. As mentioned in section 4.1, they are observed in an oval resembling the auroral oval and have been linked to ion heating, and the relationship between the BB-ELF activity and precipitating particle fluxes was quantified by Matsuoka et al. (1993). Using 5 years of data from the Cluster spacecraft, we have revisited this issue, seeking to better quantify the relationship between the BB-ELF activity and the ion flux. While Matsuoka et al. only considered the precipitating ion number flux, we have considered both the ion number and the ion energy flux, and also the upward flux of these. In addition, we have examined the location of the BB-ELF in relation to the OCB and the cusp ion dispersion region in detail. We found that the equatorward edge of the BB-ELF corresponds closely to the equatorward edge of the cusp ion dispersion region, and that its poleward edge was equatorward of the poleward edge of the cusp ion dispersion. The main result of the study, however, was the relationship between the BB-ELF and the ion fluxes. We found that the BB-ELF had a greater degree of correlation with the total field-aligned flux than with the downward flux. This was an improvement over the previous results of Matsuoka et al. (1993), and support the idea of a local ion – BB-ELF wave interaction, which has been suggested by Grison et al. (2005) and Sundkvist et al. (2005).

Paper #3: Quasistatic electric field structures and field-aligned currents in the polar cusp region

K. S. Jacobsen and J. I. Moen and A. Pedersen

The third paper investigates quasi-static electric field structures in the vicinity of the cusp. 5 years of Cluster data was examined for quasi-static electric field structures, which were then analyzed along with particle data, interplanetary magnetic field data and FAC data (calculated from magnetic field measurements). The presence of these perpendicular electric field structures at Cluster altitudes ($\sim$ 4 - 6 R_E) indicates that there is a field-aligned electric field at lower altitudes ($<$ 3.5 R_E), as the electric field strength would be impossibly large if it was mapped directly down to the ionosphere. The configuration of the electric equipotential lines linking the high altitude electric fields to the low altitude electric fields can be either S-shaped or U-shaped (See Fig. 4.1). For a U-shaped electric potential structure, the high-altitude electric field is bipolar, either converging or diverging. For an S-shaped electric potential structure, the high-altitude electric field is monopolar, pointing either poleward or equatorward. This results in four

possible configurations. We found that each of those four configurations was associated with either upward or downward current, not both. If the low altitude electric field point upwards, it will accelerate electrons downward, resulting in an inverted V and associated aurora. Previous studies have not been able to conclusively tell if dayside inverted Vs occur on closed field lines, open field lines or a combination of both (Menietti and Smith, 1993). We have found that the high altitude electric field structures accompanying inverted Vs occur exclusively on open field lines. Quasi-static electric field structures in the nightside auroral oval region has been the subject of several recent studies (e.g. Marklund et al. (2004); Johansson et al. (2006)). The dayside quasi-static electric field structures, however, have not been investigated. This paper uncovers both similarities and differences between the dayside and nightside electric field structures. In the nightside studies, monopolar electric fields were uniquely associated with the polar cap boundary while bipolar electric fields were uniquely associated with plasma boundaries within the plasma sheet. Like the previous studies, the structures found in this study coincide with plasma boundaries. The relevant boundaries at the dayside are the equatorward edge of the cusp, and the equatorward edge of injection events within the cusp. Unlike the previous studies, there is a mix of bipolar and monopolar electric fields at each of the boundaries, and there does not appear to be a connection between the type of electric field structure and the size of the density gradient across the structure. This indicates that the conditions and/or processes creating the electric field structures at the dayside are different from those at the nightside. There is a large-scale current system associated with the dayside plasma boundaries at which the electric field structures are observed. This is the cusp current system, whose direction of current is controlled by the IMF B_Y. We sorted the structures by the sign of B_Y, and found that in almost all cases the direction of the FAC associated with the structure was consistent with the expected direction of the cusp current. This indicates that the electric field structures in the dayside cusp region are generated by the cusp current system to provide the acceleration needed for the required currents to flow. A secondary result of the paper concerns the R1 current. As mentioned in section 3, the R1 current is commonly thought to flow on closed field lines, but there have been observations of R1 current flowing partially on open field lines, and some theories require part or all of the R1 current to flow on open field lines. In this paper we have for the first time documented R1 current flowing entirely on open field lines.

Future prospects

As always, unresolved questions remain. In this section I would like to share my thoughts on what kind of future works may be fruitful in further exploring the three main phenomena discussed in the papers.

Hot Flow Anomalies

Some time ago, HFAs were thought to be well understood and of little importance. Recent observations (Sibeck et al., 1998, 1999; Jacobsen et al., 2009) have discovered very strong HFAs that seriously disturb the magnetospheric boundary layers, and may eventually lead to disturbances in the ionosphere. The full importance of such events, including how frequently they occur, has not been thoroughly examined. There have been some very promising recent statistical studies of HFAs (Facsko et al., 2008, 2009), which amongst other results show that HFAs are a more common occurrence than previously thought. More work on this topic is required, perhaps combining measurements from several satellite missions to produce a sufficiently large database of HFAs. To uncover the details of how the HFAs behave and how they influence the magnetosphere, a combination of multi-spacecraft case studies and hybrid simulations should prove valuable. On a side note, the HFA phenomenon is not unique to the Earth, and was recently observed at Saturn by Masters et al. (2009).

BB-ELF

To increase our understanding of the BB-ELF phenomenon, studies of the nature of the fluctuations and their interactions with the plasma are necessary. There has been some work performed on this topic (e.g. Grison et al. (2005) and Sundkvist et al. (2005), but it is far from fully understood. Further studies will probably require a combination of theory, in-situ observations and simulation. Of particular interest are the wave modes present and the flow of energy between the plasma and the different waves. A better understanding of the underlying mechanisms will aid in determining if the BB-ELF fluctuations are indeed generated locally, and what role these fluctuations play in the heating and acceleration of the plasma.

Dayside quasistatic electric field structures

Several questions remain regarding the dayside electric field structures. Why are they sometimes monopolar and sometimes bipolar? Further studies may uncover something which we could not observe in our study. Alternatively, simulations may provide an explanation or at least show us what to look for. We assume that the potential structures are U-shaped or S-shaped, but how well does this idealized picture compare to reality? It would be interesting to compare the electric field and FAC profiles at different altitudes for the same event. This would require near-simultaneous satellite passes through the same magnetic field lines at different altitudes. Why do the equipotential lines of S-shaped potential structures always bend towards the OCB? The answer to this question may be related to the answer to the previous question. There must be something that determines the shape of the potential structure. A good place to start looking would be the ionosphere, through which the currents are closed. The local conditions in the ionosphere may set restrictions on the shape of the electric fields and currents. A study of this could be performed using a combination of data from ground radars such as EISCAT or SuperDARN and a satellite mission such as Cluster.

Bibliography

Anderson, B. J., Korth, R., Waters, C. L., Green, D. L., and Stauning, P.: Statistical Birkeland current distributions from magnetic field observations by the Iridium constellation, Annales geohpysicae, 26, 671–687, 2008.

Angelopoulos, V.: The THEMIS Mission, Space Sci. Rev., 2008.

Auster, H. U., Glassmeier, K. H., Magnes, W., Aydogar, O., Baumjohann, W., Constantinescu, D., Fischer, D., Fornacon, K. H., Georgescu, E., Harvey, P., Hillenmaier, O., Kroth, R., Ludlam, M., Narita, Y., Nakamura, R., Okrafka, K., Plaschke, F., Richter, I., Schwarzl, H., Stoll, B., Valavanoglou, A., and Wiedemann, M.: The THEMIS fluxgate magnetometer, Space Sci. Rev., 2008.

Backrud, M., Tjulin, A., Vaivads, A., Andre, M., and Fazakerley, A.: Interferometric identification of ion acoustic broadband waves in the auroral region: CLUSTER observations, GEOPHYSICAL RESEARCH LETTERS, 32, 2005.

Balogh, A., Dunlop, M., Cowley, S., Southwood, D., Thomlinson, J., Glassmeier, K., Musmann, G., Luhr, H., Buchert, S., Acuna, M., Fairfield, D., Slavin, J., Riedler, W., Schwingenschuh, K., and Kivelson, M.: The Cluster magnetic field investigation, SPACE SCIENCE REVIEWS, 79, 65–91, 1997.

Beaujardiere, O. d. l., Watermann, J., Newell, P., and Rich, F.: Relationship between Birkeland current regions, particle-precipitation, and electric-fields, Journal of geophysical research-Space physics, 98, 7711–7720, 1993.

Birkeland, K.: The Norwegian Aurora Polaris Expedition 1902-1903, vol. 1, H. Aschehoug & Co., 1908.

Bogdanova, Y., Fazakerley, A., Owen, C., Klecker, B., Cornilleau-Wehrlin, N., Grison, B., Andre, M., Cargill, P., Reme, H., Bosqued, J., Kistler, L., and Balogh, A.: Correlation between suprathermal electron bursts, broadband extremely low frequency waves, and local ion heating in the midaltitude cleft/low-latitude boundary layer observed by Cluster, JOURNAL OF GEOPHYSICAL RESEARCH-SPACE PHYSICS, 109, 2004.

Borg, A. L., Ostgaard, N., Pedersen, A., Oieroset, M., Phan, T. D., Germany, G., Aasnes, A., Lewis, W., Stadsnes, J., Lucek, E. A., Reme, H., and Mouikis, C.: Simultaneous observations of magnetotail reconnection and bright X-ray aurora on 2 October 2002, Journal of geophysical research-Space physics, 112, 2007.

Bouhram, M., Dubouloz, N., Malingre, M., Jasperse, J., Pottelette, R., Senior, C., Delcourt, D., Carlson, C., Roth, I., Berthomier, M., and Sauvaud, J.: Ion outflow and associated perpendicular heating in the cusp observed by Interball Auroral Probe and Fast Auroral Snapshot, Journal of geophysical research-Space physics, 107, 2002.

Burchill, J., Knudsen, D., Bock, B., Pfaff, R., Wallis, D., Clemmons, J., Bounds, S., and Stenbaek-Nielsen, H.: Core ion interactions with BB ELF, lower hybrid, and Alfven waves in the high-latitude topside ionosphere, JOURNAL OF GEOPHYSICAL RESEARCH-SPACE PHYSICS, 109, 2004.

Burgess, D.: On the effect of a tangential discontinuity on ions specularly reflected at an oblique shock, Journal of geophysical research-space physics, 94, 472–478, 1989.

Burgess, D. and Schwartz, S.: Colliding plasma structures - current sheet and perpendicular shock, Journal of geophysical research-space physics, 93, 11 327–11 340, 1988.

Carlqvist, P. and Bostrom, R.: Space-charge regions above aurora, Journal of geophysical research, 75, 7140–&, 1970.

Cowley, S.: Magnetosphere-ionosphere interactions: A tutorial review, in MAGNETO-SPHERIC CURRENT SYSTEMS, edited by Ohtani, S and Fujii, R and Hesse, M and Lysak, RL, vol. 118 of *GEOPHYSICAL MONOGRAPH SERIES*, pp. 91–106, Amer Geophys Union; Natl Sci Fdn; NASA; USN Off Naval Res, AMER GEOPHYSICAL UNION, 2000 FLORIDA AVE NW, WASHINGTON, DC 20009 USA, Conference on Magnetospheric Current Systems, KONA, HI, JAN 10-15, 1999, 2000.

Credland, J. and Schmidt, R.: The resurrection of the cluster scientific mission, ESA BULLETIN-EUROPEAN SPACE AGENCY, pp. 5–10, 1997.

Credland, J., Mecke, G., and Ellwood, J.: The Cluster mission: ESA's spacefleet to the magnetosphere, SPACE SCIENCE REVIEWS, 79, 33–64, 1997.

Cummings, W. D. and Dessler, A. J.: Field-Aligned Currents in the Magnetosphere, Journal of geophysical research, 72, 1007–1013, 1967.

Eastwood, J. P., Sibeck, D. G., Angelopoulos, V., Phan, T. D., Bale, S. D., McFadden, J. P., Cully, C. M., Mende, S. B., Larson, D., Frey, S., Carlson, C. W., Glassmeier, K.-H., Auster, H. U., Roux, A., and Contel, O. L.: THEMIS observations of a hot flow anomaly: Solar wind, magnetosheath, and ground-based measurements, Geophys. Res. Lett., 35, 2008.

Facsko, G., Kecskemety, K., Erdos, G., Tatrallyay, M., Daly, P. W., and Dandouras, I.: A statistical study of hot flow anomalies using Cluster data, Advances in space research, 41, 1286–1291, 2008.

Facsko, G., Nemeth, Z., Erdos, G., Kis, A., and Dandouras, I.: A global study of hot flow anomalies using Cluster multi-spacecraft measurements, Annales geophysicae, 27, 2057–2076, 2009.

Glassmeier, K. H.: TRAVELING MAGNETOSPHERIC CONVECTION TWIN-VORTICES - OBSERVATIONS AND THEORY, Ann. Geophys., 10, 547–565, 1992.

Green, D. L., Waters, C. L., Anderson, B. J., and Korth, H.: Seasonal and interplanetary magnetic field dependence of the field-aligned currents for both Northern and Southern Hemispheres, Annales geophysicae, 27, 1701–1715, 2009.

Grison, B., Sahraoui, F., Lavraud, B., Chust, T., Cornilleau-Wehrlin, N., Reme, H., Balogh, A., and Andre, M.: Wave particle interactions in the high-altitude polar cusp: a Cluster case study, ANNALES GEOPHYSICAE, 23, 3699–3713, 2005.

Gurnett, D. and Frank, L.: REGION OF INTENSE PLASMA-WAVE TURBULENCE ON AURORAL FIELD LINES, JOURNAL OF GEOPHYSICAL RESEARCH-SPACE PHYSICS, 82, 1031–1050, 1977.

Gurnett, D., Huff, R., Menietti, J., Burch, J., Winningham, J., and Shawhan, S.: CORRELATED LOW-FREQUENCY ELECTRIC AND MAGNETIC NOISE ALONG THE AURORAL FIELD LINES, JOURNAL OF GEOPHYSICAL RESEARCH-SPACE PHYSICS, 89, 8971–8985, 1984.

Gustafsson, G., Bostrom, R., Holback, B., Holmgren, G., Lundgren, A., Stasiewicz, K., Ahlen, L., Mozer, F., Pankow, D., Harvey, P., Berg, P., Ulrich, R., Pedersen, A., Schmidt, R., Butler, A., Fransen, A., Klinge, D., Thomsen, M., Falthammar, C., Lindqvist, P., Christenson, S., Holtet, J., Lybekk, B., Sten, T., Tanskanen, P., Lappalainen, K., and Wygant, J.: The electric field and wave experiment for the Cluster mission, SPACE SCIENCE REVIEWS, 79, 137–156, 1997.

Hamrin, M., Norqvist, P., Hellstrom, T., Andre, M., and Eriksson, A.: A statistical study of ion energization at 1700 km in the auroral region, ANNALES GEOPHYSICAE, 20, 1943–1958, 2002.

Hamrin, M., Marghitu, O., Ronnmark, K., Klecker, B., Andre, M., Buchert, S., Kistler, L., McFadden, J., Reme, H., and Vaivads, A.: Observations of concentrated generator regions in the nightside magnetosphere by Cluster/FAST conjunctions, Annales geophysicae, 24, 637–649, 2006.

Iijima, T. and Potemra, T.: Amplitude distribution of field-aligned currents at northern high latitudes observed by Triad, Journal of geophysical research-Space physics, 81, 2165–2174, 1976a.

Iijima, T. and Potemra, T.: Field-aligned currents in dayside cusp observed by Triad, Journal of geophysical research-Space physics, 81, 5971–5979, 1976b.

Iijima, T., Fujii, R., Potemra, T., and Saflekos, N.: Field-aligned currents in south polar cusp and their relationship to inter-planetary magnetic-field, Journal of geophysical research-Space physics, 83, 5595–5603, 1978.

Ivchenko, N. and Marklund, G.: Observation of low frequency electromagnetic activity at 1000 km altitude, ANNALES GEOPHYSICAE, 19, 643–648, 2001.

Jacobsen, K. S., Phan, T. D., Eastwood, J. P., Sibeck, D. G., Moen, J. I., Angelopoulos, V., McFadden, J. P., Engebretson, M. J., Provan, G., Larson, D., and Fornacon, K. H.: THEMIS observations of extreme magnetopause motion caused by a hot flow anomaly, Journal of geophysical research-Space physics, 114, 2009.

Johansson, T., Marklund, G., Karlsson, T., Lileo, S., Lindqvist, P. A., Marchaudon, A., Nilsson, H., and Fazakerley, A.: On the profile of intense high-altitude auroral electric fields at magnetospheric boundaries, ANNALES GEOPHYSICAE, 24, 1713–1723, 2006.

Johnstone, A., Alsop, C., Burge, S., Carter, P., Coates, A., Coker, A., Fazakerley, A., Grande, M., Gowen, R., Gurgiolo, C., Hancock, B., Narheim, B., Preece, A., Sheather, P., Winningham, J., and Woodliffe, R.: Peace: A plasma electron and current experiment, SPACE SCIENCE REVIEWS, 79, 351–398, 1997.

Juusola, L., Kauristie, K., Amm, O., and Ritter, P.: Statistical dependence of auroral ionospheric currents on solar wind and geomagnetic parameters from 5 years of CHAMP satellite data, Annales geophysicae, 27, 1005–1017, 2009.

Kasahara, Y., Hosoda, T., Mukai, T., Watanabe, S., Kimura, I., Kojima, H., and Niitsu, R.: ELF/VLF waves correlated with transversely accelerated ions in the auroral region observed by Akebono, JOURNAL OF GEOPHYSICAL RESEARCH-SPACE PHYSICS, 106, 21 123–21 136, 2001.

Kataoka, R., Fukunishi, H., Lanzerotti, L. J., Rosenberg, T. J., Weatherwax, A. T., Engebretson, M. J., and Watermann, J.: Traveling convection vortices induced by solar wind tangential discontinuities, J. Geophys. Res., 107, 1455, 2002.

Kintner, P., Bonnell, J., Arnoldy, R., Lynch, K., Pollock, C., and Moore, T.: SCIFER - Transverse ion acceleration and plasma waves, GEOPHYSICAL RESEARCH LETTERS, 23, 1873–1876, 1996.

Kintner, P., Franz, J., Schuck, P., and Klatt, E.: Interferometric coherency determination of wavelength or what are broadband ELF waves?, JOURNAL OF GEOPHYSICAL RESEARCH-SPACE PHYSICS, 105, 21 237–21 250, 2000.

Kivelson, M. G. and Russell, C. T.: Introduction to space physics, Cambridge university press, 1995.

Knight, S.: Parallel electric-fields, Planetary and space science, 21, 741–750, 1973.

Knudsen, D., Clemmons, J., and Wahlund, J.: Correlation between core ion energization, suprathermal electron bursts, and broadband ELF plasma waves, JOURNAL OF GEOPHYSICAL RESEARCH-SPACE PHYSICS, 103, 4171–4186, 1998.

Lin, C. and Hoffman, R.: Observations of inverted-V electron-precipitation, Space science reviews, 33, 415–457, 1982.

Lin, Y.: Global hybrid simulation of hot flow anomalies near the bow shock and in the magnetosheath, Planetary and space science, 50, 577–591, Symposium on Intercomparative Magetosheath Studies, ANTALYA, TURKEY, SEP 04-08, 2000, 2002.

Lopez, R. E., Hernandez, S., Hallman, K., Valenzuela, R., Seller, J., Anderson, P. C., and Hairston, M. R.: Field-aligned currents in the polar cap during saturation of the polar cap potential, Journal of atmospheric and solar-terrestrial physics, 70, 555–563, International Symposium on Recent Observations and Simulations of the Sun-Earth System (ISROSES), Varna, BULGARIA, SEP 17-22, 2006, 2008.

Luhmann, J. and Brace, L.: Near-Mars space, Reviews of geophysics, 29, 121–140, 1991.

Lund, E., Mobius, E., Carlson, C., Ergun, R., Kistler, L., Klecker, B., Klumpar, D., McFadden, J., Popecki, M., Strangeway, R., and Tung, Y.: Transverse ion acceleration mechanisms in the aurora at solar minimum: occurrence distributions, JOURNAL OF ATMOSPHERIC AND SOLAR-TERRESTRIAL PHYSICS, 62, 467–475, 2000.

Lundin, R. and Eliasson, L.: Auroral energization processes, Annales geophysicae-Atmospheres hydrospheres and space sciences, 9, 202–223, SYMP OF THE 15TH MEETING OF THE EUROPEAN GEOPHYSICAL SOC : ACCELERATION AND HEATING PROCESSES IN SOLAR SYSTEM PLASMAS, COPENHAGEN, DENMARK, APR 23-27, 1990, 1991.

Lynch, K., Bonnell, J., Carlson, C., and Peria, W.: Return current region aurora: E-parallel to, j(z), particle energization, and broadband ELF wave activity, JOURNAL OF GEOPHYSICAL RESEARCH-SPACE PHYSICS, 107, 2002.

Lyons, L.: Generation of large-scale regions of auroral currents, electric potentials, and precipitation by the divergence of the convection electric-field, Journal of geophysical research-Space physics, 85, 17–24, 1980.

Maggiolo, R., Sauvaud, J. A., Fontaine, D., Teste, A., Grigorenko, E., Balogh, A., Fazakerley, A., Paschmann, G., Delcourt, D., and Reme, H.: A multi-satellite study of accelerated ionospheric ion beams above the polar cap, Annales geophysicae, 24, 1665–1684, 2006.

Marklund, G., Blomberg, L., Falthammar, C., Erlandson, R., and Potemra, T.: SIGNATURES OF THE HIGH-ALTITUDE POLAR CUSP AND DAYSIDE AURORAL REGIONS AS SEEN BY THE VIKING ELECTRIC-FIELD EXPERIMENT, JOURNAL OF GEOPHYSICAL RESEARCH-SPACE PHYSICS, 95, 5767–5780, 1990.

Marklund, G. T., Karlsson, T., Figueiredo, S., Johansson, T., Lindqvist, P.-A., André, M., Buchert, S., Kistler, L. M., and Fazakerley, A.: Characteristics of quasi-static potential structures observed in the auroral return current region by Cluster, Nonlinear Processes in Geophysics, 11, 709–720, http://www.nonlin-processes-geophys.net/11/709/2004/, 2004.

Masters, A., McAndrews, H. J., Steinberg, J. T., Thomsen, M. F., Arridge, C. S., Dougherty, M. K., Billingham, L., Schwartz, S. J., Sergis, N., Hospodarsky, G. B., and Coates, A. J.: Hot

flow anomalies at Saturn's bow shock, Journal of geophysical research-Space physics, 114, 2009.

Matsuoka, A., Mukai, T., Hayakawa, H., Kohno, Y., Tsuruda, K., Nishida, A., Okada, T., Kaya, N., and Fukunishi, H.: EXOS-D OBSERVATIONS OF ELECTRIC-FIELD FLUCTU-ATIONS AND CHARGED-PARTICLE PRECIPITATION IN THE POLAR CUSP, GEO-PHYSICAL RESEARCH LETTERS, 18, 305–308, 1991.

Matsuoka, A., Tsuruda, K., Hayakawa, H., Mukai, T., Nishida, A., Okada, T., Kaya, N., and Fukunishi, H.: ELECTRIC-FIELD FLUCTUATIONS AND CHARGED-PARTICLE PRECIPITATION IN THE CUSP, JOURNAL OF GEOPHYSICAL RESEARCH-SPACE PHYSICS, 98, 11 225–11 234, 1993.

Maynard, N., Heppner, J., and Egeland, A.: INTENSE, VARIABLE ELECTRIC-FIELDS AT IONOSPHERIC ALTITUDES IN THE HIGH-LATITUDE REGIONS AS OBSERVED BY DE-2, GEOPHYSICAL RESEARCH LETTERS, 9, 981–984, 1982.

McDiarmid, I., Burrows, J., and Wilson, M.: Magnetic-field perturbations in dayside cleft and their relationship to IMF, Journal of geophysical research-Space physics, 83, 5753–5756, 1978.

McFadden, J., Carlson, C., and Ergun, R.: Microstructure of the auroral acceleration region as observed by FAST, Journal of geophysical research-Space physics, 104, 14 453–14 480, Meeting on the Interrelationship Between Plasma Experiments in the Laboratory and in Space, MAUI, HAWAII, 1997, 1999.

McFadden, J. P., Carlson, C. W., Larson, D., Ludlam, M., Abiad, R., Elliott, B., Turin, P., Marckwordt, M., and Angelopoulos, V.: The THEMIS ESA Plasma Instrument and In-flight Calibration, SPACE SCIENCE REVIEWS, 141, 277–302, 2008.

Mende, S. B., Harris, S. E., Frey, H. U., Angelopoulos, V., Russell, C. T., Donovan, E., Jackel, B., Greffen, M., and Peticolas, L. M.: The THEMIS array of ground based observatories for the study of auroral substorms, Space Sci. Rev., 2008.

Menietti, J. and Smith, M.: Inverted Vs spanning the cusp boundary-layer, Journal of geophys-ical research-Space physics, 98, 11 391–11 400, 1993.

Miyake, W., Matsuoka, A., and Hirano, Y.: A statistical survey of low-frequency electric field fluctuations around the dayside cusp/cleft region, JOURNAL OF GEOPHYSICAL RESEARCH-SPACE PHYSICS, 108, 2003.

Mozer, F. and Hull, A.: Origin and geometry of upward parallel electric fields in the auroral acceleration region, Journal of geophysical research-Space physics, 106, 5763–5778, 2001.

Mozer, F., Cattell, C., Hudson, M., Lysak, R., Temerin, M., and Torbert, R.: Satellite measure-ments and theories of low altitude auroral particle-acceleration, Space science reviews, 27, 155–213, 1980.

Olsson, A. and Janhunen, P.: Some recent developments in understanding auroral electron acceleration processes, IEEE transactions on plasma science, 31, 1178–1191, 2003.

Reme, H., Bosqued, J., Sauvaud, J., Cros, A., Dandouras, J., Aoustin, C., Bouyssou, J., Camus, T., Cuvilo, J., Martz, C., Medale, J., Perrier, H., Romefort, D., Rouzaud, J., dUston, C., Mobius, E., Crocker, K., Granoff, M., Kistler, L., Popecki, M., Hovestadt, D., Klecker, B., Paschmann, G., Scholer, M., Carlson, C., Curtis, D., Lin, R., McFadden, J., Formisano, V., Amata, E., BavassanoCattaneo, M., Baldetti, P., Belluci, G., Bruno, R., Chionchio, G., DiLellis, A., Shelley, E., Ghielmetti, A., Lennartsson, W., Korth, A., Rosenbauer, H., Lundin, R., Olsen, S., Parks, G., McCarthy, M., and Balsiger, H.: The Cluster ion spectrometry (CIS) experiment, SPACE SCIENCE REVIEWS, 79, 303–350, 1997.

Russell, C. T., Chi, P. J., Dearborn, D. J., Ge, Y. S., Kuo-Tiong, B., Means, J. D., Pierce, D. R., Rowe, K. M., and Snare, R. C.: THEMIS ground-based magnetometers, Space Sci. Rev., 2008.

Schwartz, S. J. and et al.: An active current sheet in the solar wind, Nature, 318, 269–271, 1985.

Schwartz, S. J., Paschmann, G., Sckopke, N., Bauer, T. M., Dunlop, M., Fazakerley, A. N., and Thomsen, M. F.: Conditions for the formation of hot flow anomalies at Earth's bow shock, J. Geophys. Res., 105, 12 639–12 650, 2000.

Sibeck, D., Borodkova, N., Zastenker, G., Romanov, S., and Sauvaud, J.: Gross deformation of the dayside magnetopause, GEOPHYSICAL RESEARCH LETTERS, 25, 453–456, 1998.

Sibeck, D. G., Borodkova, N. L., Schwartz, S. J., Owen, C. J., Kessel, R., Kokubun, S., Lepping, R. P., Lin, R., Liou, K., Lühr, H., McEntire, R. W., Meng, C.-I., Mukai, T., Nemecek, Z., Parks, G., Phan, T. D., Romanov, S. A., Safrankova, J., Sauvaud, J.-A., Singer, H. J., Solovyev, S. I., Szabo, A., Takahashi, K., Williams, D. J., Yumoto, K., and Zastenker, G. N.: Comprehensive study of the magnetospheric response to a hot flow anomaly, J. Geophy. Res., 104, 4577–4593, 1999.

Sibeck, D. G., Kudela, K., Lepping, R. P., Lin, R., Nemecek, Z., Nozdrachev, M. N., Phan, T. D., Prech, L., Safrankova, J., Singer, H., and Yermolaev, Y.: Magnetopause motion driven by interplanetary magnetic field variations, J. Geophys. Res., 105, 25 155–25 169, 2000.

Siscoe, G., Crooker, N., and Siebert, K.: Transpolar potential saturation: Roles of region 1 current system and solar wind ram pressure, JOURNAL OF GEOPHYSICAL RESEARCH-SPACE PHYSICS, 107, 2002a.

Siscoe, G., Erickson, G., Sonnerup, B., Maynard, N., Schoendorf, J., Siebert, K., Wiemer, D., White, W., and Wilson, G.: Hill model of transpolar potential saturation: Comparisons with MHD simulations, JOURNAL OF GEOPHYSICAL RESEARCH-SPACE PHYSICS, 107, 2002b.

Siscoe, G. L.: Global force balance of region 1 current system, Journal of atmospheric and solar-terrestrial physics, 68, 2119–2126, 2006.

Stasiewicz, K., Lundin, R., and Marklund, G.: Stochastic ion heating by orbit chaotization on electrostatic waves and nonlinear structures, PHYSICA SCRIPTA, T84, 60–63, International Topical Conference on Plasma Physics - New Frontiers in Nonlinear Sciences, FARO, POR-TUGAL, SEP 06-10, 1999, 2000.

Stern, D.: The origins of Birkeland currents, Reviews of geophysics, 21, 125–138, 1983.

Stone, E., Frandsen, A., Mewaldt, R., Christian, E., Margolies, D., Ormes, J., and Snow, F.: The Advanced Composition Explorer, Space science reviews, 86, 1–22, 1998.

Sugiura, M., Maynard, N., Farthing, W., Heppner, J., Ledley, B., and Cahill, L.: INITIAL RESULTS ON THE CORRELATION BETWEEN THE MAGNETIC AND ELECTRIC-FIELDS OBSERVED FROM THE DE-2 SATELLITE IN THE FIELD-ALIGNED CUR-RENT REGIONS, GEOPHYSICAL RESEARCH LETTERS, 9, 985–988, 1982.

Sundkvist, D., Vaivads, A., Andre, M., Wahlund, J., Hobara, Y., Joko, S., Krasnoselskikh, V., Bogdanova, Y., Buchert, S., Cornilleau-Wehrlin, N., Fazakerley, A., Hall, J., Reme, H., and Stenberg, G.: Multi-spacecraft determination of wave characteristics near the proton gyrofrequency in high-altitude cusp, ANNALES GEOPHYSICAE, 23, 983–995, 2005.

Taguchi, S., Sugiura, M., Winningham, J., and Slavin, J.: Characterization of the IMF By-dependent field-aligned currents in the cleft region based on DE-2 observations, Journal of geophysical research-Space physics, 98, 1393–1407, 1993.

Tam, S., Chang, T., Kintner, P., and Klatt, E.: Intermittency analyses on the SIERRA measurements of the electric field fluctuations in the auroral zone, GEOPHYSICAL RESEARCH LETTERS, 32, 2005.

Thomsen, M. F., Gosling, J. T., Fuselier, S. A., Bame, S. J., and Russell, C. T.: Hot, diamagnetic cavities upstream from the Earth's bow shock, J. Geophys. Res., 91, 2961–2973, 1986.

Thomsen, M. F., Thomas, V. A., Winske, D., Gosling, J. T., Farris, M. H., and Russell, C. T.: Observational test of hot flow anomaly formation by the interaction of a magnetic disconti-nuity with the bow shock, J. Geophys. Res., 98, 15 319–15 330, 1993.

Wahlund, J., Eriksson, A., Holback, B., Boehm, M., Bonnell, J., Kintner, P., Seyler, C., Clem-mons, J., Eliasson, L., Knudsen, D., Norqvist, P., and Zanetti, L.: Broadband ELF plasma emission during auroral energization 1. Slow ion acoustic waves, JOURNAL OF GEOPHYS-ICAL RESEARCH-SPACE PHYSICS, 103, 4343–4375, 1998.

Wilhjelm, J., Friischristensen, E., and Potemra, T.: Relationship between ionospheric and field-aligned currents in dayside cusp, Journal of geophysical research-Space physics, 83, 5586–5594, 1978.

Wilken, B., Axford, W., Daglis, I., Daly, P., Guttler, W., Ip, W., Korth, A., Kremser, G., Livi, S., Vasyliunas, V., Woch, J., Baker, D., Belian, R., Blake, J., Fennell, J., Lyons, L., Borg, H., Fritz, T., Gliem, F., Rathje, R., Grande, M., Hall, D., Kecsuemety, K., McKennaLawlor, S., Mursula, K., Tanskanen, P., Pu, Z., Sandahl, I., Sarris, E., Scholer, M., Schulz, M., Sorass, F.,

and Ullaland, S.: RAPID - The imaging energetic particle spectrometer on Cluster, SPACE SCIENCE REVIEWS, 79, 399–473, 1997.

Xu, D. and Kivelson, M.: Polar-cap field-aligned currents for southward interplanetary magnetic-fields, Journal of geophysical research-Space physics, 99, 6067–6078, 1994.

Zmuda, A., Martin, J., and Heuring, F.: Transverse magnetic disturbances at 1100 kilometers in auroral region, Journal of geophysical research, 71, 5033–&, 1966.

Click Here for Full Article

THEMIS observations of extreme magnetopause motion caused by a hot flow anomaly

K. S. Jacobsen,[1] T. D. Phan,[2] J. P. Eastwood,[2] D. G. Sibeck,[3] J. I. Moen,[1]
V. Angelopoulos,[4] J. P. McFadden,[2] M. J. Engebretson,[5] G. Provan,[6]
D. Larson,[2] and K.-H. Fornaçon[7]

[1] On 30 October 2007, the five THEMIS spacecraft observed the cause and consequence of extreme motion of the dawn flank magnetopause, displacing the magnetopause outward by at least 4.8 R_E in 59 s, with flow speeds in the direction normal to the model magnetopause reaching 800 km/s. While the THEMIS A, C, D, and E observations allowed the determination of the velocity, size, and shape of a large bulge moving tailward along the magnetopause at a speed of 355 km/s, THEMIS B observed the signatures of a hot flow anomaly (HFA) upstream of the bow shock at the same time, indicating that the pressure perturbation generated by the HFA may be the source of the fast compression and expansion of the magnetosphere. The transient deformation of the magnetopause generated field-aligned currents and created traveling convection vortices which were detected by ground magnetometers. This event demonstrates that kinetic (non-MHD) effects at the bow shock can have global consequences on the magnetosphere.

Citation: Jacobsen, K. S., et al. (2009), THEMIS observations of extreme magnetopause motion caused by a hot flow anomaly, *J. Geophys. Res.*, *114*, A08210, doi:10.1029/2008JA013873.

1. Introduction

[2] It is well known that the magnetopause moves and changes in response to varying solar wind conditions. Several studies have been conducted to determine the typical thickness and speed of the magnetopause for different solar wind conditions [e.g., *Berchem and Russell*, 1982; *Le and Russell*, 1994; *Paschmann et al.*, 1993]. *Phan and Paschmann* [1996] found average velocities of the magnetopause in the direction normal to the magnetopause to be 40 km/s or less, with a maximum recorded value of 162 km/s. *Winterhalter et al.* [1981] also observed a magnetopause speed of 195 km/s, and *Sibeck* [1995] reported a speed of 300 km/s. The most obvious cause of this kind of motion is pressure variation in the solar wind, but it can also result from nonlinear interaction in the boundary layers upstream of the Earth's magnetosphere.

[3] In particular, a discontinuity in the solar wind magnetic field hitting the bow shock will for certain field configurations cause a violent reaction, known as a hot flow anomaly (HFA), that creates strong density variations, plasma heating and flow deflections. As the disturbance propagates downstream, it will cause magnetopause motion. More information about HFAs is presented in section 2.

[4] Transient magnetopause deformations can cause ground signatures as they move tailward, as described by *Glassmeier* [1992] and *Kataoka et al.* [2002]. Deformations of the magnetopause cause field-aligned currents that in turn create Traveling Convection Vortices (TCV), which are detected as Magnetic Impulse Events (MIE) by magnetometers on the ground.

[5] The observations presented in this paper show magnetopause motion of large amplitude and a much greater speed than previously seen. Through multispacecraft observations we are able to infer the shape of the deformed magnetopause. Observations of the pristine solar wind by ACE and the solar wind just upstream of the dawn bow shock by THEMIS B reveal the cause for the drastic magnetopause motion, and ground observations provide complementary information on the deformation of the magnetopause.

2. Hot Flow Anomalies

[6] HFAs were first discovered in the mid-1980s, in association with the passage of interplanetary current sheets [*Schwartz et al.*, 1985; *Thomsen et al.*, 1986] A number of simulations were performed, exploring different theoretical explanations for the phenomenon. *Burgess and Schwartz* [1988] found that a magnetic field reversal convecting into a shock led to overreflection followed by upstream penetration of ions from the shock. The reflected ions are thermal-

[1]Department of Physics, University of Oslo, Oslo, Norway.
[2]Space Sciences Laboratory, University of California, Berkeley, California, USA.
[3]NASA Goddard Space Flight Center, Greenbelt, Maryland, USA.
[4]IGPP, ESS, University of California, Los Angeles, California, USA.
[5]Department of Physics, Augsburg College, Minneapolis, Minnesota, USA.
[6]Department of Physics and Astronomy, University of Leicester, Leicester, UK.
[7]IGEP, Technische Universität Braunschweig, Braunschweig, Germany.

ized through ion beam instabilities. *Burgess* [1989] investigated the role of the convection electric field ($-\mathbf{V} \times \mathbf{B}$) and found that a convection electric field pointing toward the discontinuity is necessary to focus the reflected ions into the discontinuity. *Thomsen et al.* [1993] provided an observational test of the importance of the convection electric field, which confirmed the results of the simulations by Burgess.

[7] *Schwartz* [1995] reviewed the current knowledge of HFAs and summarized the observational characteristics, of which the main points were as follows:

[8] 1. The events are flanked by regions of enhanced magnetic field strength, plasma density, and a slight increase in temperature. Sometimes only one edge shows these characteristics.

[9] 2. The central regions of HFAs contain hot (10^6–10^7 K) plasma that is flowing significantly slower than the ambient solar wind and is highly deflected from the Sun-Earth line. The magnetic field drops, and the density is at or below solar wind values.

[10] 3. HFAs are found associated with gross changes in the IMF direction.

[11] 4. HFAs convect with the solar wind flow.

[12] Interest in HFAs was renewed in the late 1990s, as observations were made of a large magnetopause deformation associated with a HFA [*Sibeck et al.*, 1998, 1999]. They found an outward movement of 5 Earth radii (R_E) in 7 min resulting from a HFA. *Schwartz et al.* [2000] performed a study of 30 HFAs, and amongst other results, calculated an occurrence rate of 3 per day. These results indicate that HFAs are more common and have a far greater influence on the magnetosphere than previously thought. *Sibeck et al.* [2000] further investigated HFAs, and a short summary of their conceptual HFA model can be seen in Figure 1 of that paper.

[13] The most recent theoretical work on HFAs is a hybrid simulation by *Lin* [2002], in which she studied the formation and structure of strong HFAs at the bow shock and in the magnetosheath, and their effects on the magnetopause. A statistical study of HFAs using data from the Cluster mission confirmed some of the predictions from that simulation, and presented evidence that fast solar wind is an essential condition for HFA formation [*Facsko et al.*, 2008].

[14] *Eastwood et al.* [2008] observed a HFA both up and downstream of the bow shock simultaneously. They noted that the resulting pressure perturbation would cause a significant shift in the magnetopause location but no direct observations of the magnetopause were available in that event.

[15] To summarize, a HFA is generated when a discontinuity in the solar wind magnetic field hits the bow shock under certain conditions. The most important condition is that the convection electric field points toward the discontinuity on at least one side. Ions reflected from the bow shock are focused into the discontinuity, where they thermalize through ion beam instabilities. This causes plasma pressure to rise, which in turn leads to an expansion of the heated plasma into the ambient plasmas both upstream and downstream of the bow shock. This expansion leads to a drop in density and magnetic field strength, and may compress plasma and magnetic field on one or both sides of the expanded area. It also causes a change in the local plasma flow, which may even become sunward in some cases. This structure is what is detected as a HFA. A strong HFA will propagate through the magnetosheath and hit the magnetopause, at which point the variations in ram pressure will cause the magnetosphere to compress or expand as the regions of enhanced and depleted density arrive.

3. Orbits and Instrumentation

[16] On 30 October 2007 THEMIS [*Angelopoulos*, 2008] was in the orbit placement stage of its mission, and the spacecraft were approximately aligned along the GSM Y axis with smaller differences in X and Z. As shown in Figure 1, THEMIS A, D and E were just inside the magnetosphere, C was in the magnetosheath, and B was in the solar wind. All spacecraft were moving at less than 2 km/s, which is negligible for the phenomenon described in this paper. Data from the fluxgate magnetometer (FGM) [*Auster et al.*, 2008] and the electrostatic plasma analyzer (ESA) [*McFadden et al.*, 2008] are used. For the solar wind observations, the THEMIS B ESA was in the 32 energy sweeps/spin mode, which does not fully resolve the narrow solar wind beam. Thus the absolute values of the solar wind ion moments and their variations should be considered qualitative.

4. Observations
4.1. Magnetopause Observations

[17] Figure 2 shows data from the magnetic field experiment (FGM) and the thermal plasma instrument (ESA) for THEMIS A, C, D and E. At 1404:55 UT, THEMIS D entered the magnetosheath. It remained in the magnetosheath until 1406:20 UT, and immediately after exiting it, a velocity of 800 km/s normal to the model magnetopause [*Fairfield*, 1971] was observed. This is much larger than previously reported values for magnetopause motion.

[18] To place this observation in context, the order of the spacecraft shown in Figure 2 is sorted by the spacecraft distance from the model magnetopause. THEMIS C was in the magnetosheath, the rest were inside the magnetopause. A was the closest spacecraft to the model magnetopause, followed by D, then E. Spacecraft A, D and E all had brief encounters with the magnetosheath, but not in the order of proximity to the magnetopause, which means that this was not a one-dimensional large-scale compression of the magnetosphere. Instead, entry into the magnetosheath was ordered by position in X_{GSE}. Spacecraft D entered first, followed in succession by E and A, located further down the flank. This suggests that there was an inward deformation of the magnetopause which progressed tailward. Assuming that this is true, and that the large-scale shape of the inward bulge did not change much as it passed by A, D and E, we can estimate its velocity along the magnetopause. We use the middle of the magnetosheath encounters for these calculations, as the bulge width decreases with increasing distance from the magnetopause, but the center should remain approximately the same. Dividing the distance tailward along the model magnetopause from one magnetosheath encounter to another by the time difference, we obtain the values shown in Table 1. The speed of the bulge is remarkably similar for the 3 spacecraft pairs, with an average of 355 km/s. Multiplying the velocity by the
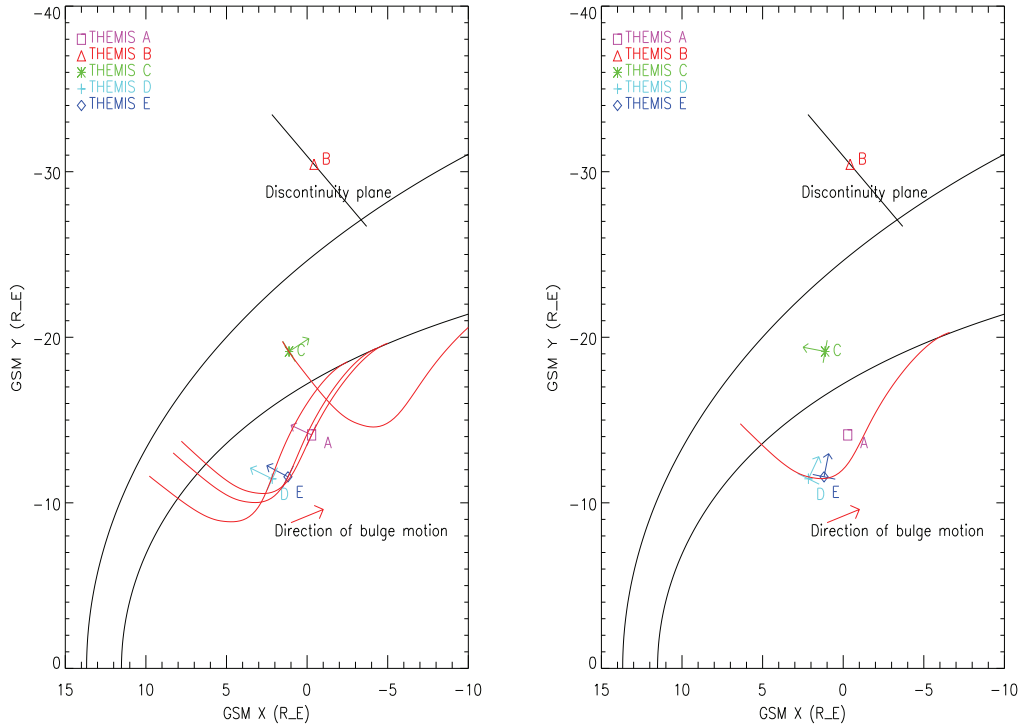
Figure 1. (left) Magnetopause [*Shue et al.*, 1997], bow shock [*Farris et al.*, 1991; *Cairns et al.*, 1995], positions of the THEMIS spacecraft, and the orientation of the discontinuity plane in the solar wind are shown, together with normals for the first magnetopause crossing for each of the spacecraft, and drawings of the magnetopause bulge. (right) The same as Figure 1 (left), but normals for each spacecraft's second magnetopause crossing are shown together with the inferred magnetopause.

magnetosheath encounter durations, we obtain a measure of the width of the bulge along the model magnetopause at different distances to the model magnetopause. The width of the bulge is 6.1 R_E for A, 4.7 R_E for D, and 2.8 R_E for E.

[19] At 1407:30 UT THEMIS A entered the magnetosphere and at 1408:35 UT the magnetic field observations of THEMIS C indicate that it also entered the magnetosphere. The spacecraft were separated by 4.77 R_E in the normal direction but only 0.32 R_E tailward along the model magnetopause. This separation makes them well suited to get an estimate for the amplitude and speed of the magnetopause in the direction normal to the model magnetopause. Using the estimated velocity of the bulge tailward, we subtract 6 s from the time interval to account for the distance along the model magnetopause. The magnetopause moved outward at least 4.77 R_E in less than 59 s, which gives an average velocity normal to the model magnetopause of at least 515 km/s for this time interval. This agrees with the plasma measurements, which detected velocities normal to the model magnetopause of approximately 300, 800 and 600 km/s for THEMIS A, D and E (Figures 2c, 2f, and 2i).

[20] Performing the minimum variance analysis (MVA) [*Sonnerup and Cahill*, 1967] on the magnetic field data of

each spacecraft for each crossing into and out of the magnetosheath, we find the normals of the actual magnetopause. For THEMIS A, D and E, the normals for the first crossings are all well defined, with intermediate-to-minimum eigenvalue ratios greater than 10. The rest of the normals are reasonably well defined, with eigenvalue ratios of at least 4. The magnetic field sampling frequency was $\frac{1}{3}$ Hz for THEMIS C, and 4 Hz for the other spacecraft. The results of MVA may vary with the length of the time interval chosen for analysis. If the results vary greatly for different time intervals, they are unreliable. Because of this, intervals with lengths ranging from 10 to 120 s were examined. The time intervals used for the final values range from 20 to 35 s for the different spacecraft. The normal for the second crossing of THEMIS A changes significantly when using different time intervals for the MVA analysis, which indicates that it cannot be trusted.

[21] Using these normals and the estimated values above, we reconstruct the shape of the bulge on the magnetopause. The result is seen in Figure 1. On the left the MVA normals for the first crossings are shown together with drawings of the bulge, and the normals for the second crossings are shown on the right. THEMIS A, D and E first crossed the magnetopause going from the magnetosphere to the mag-
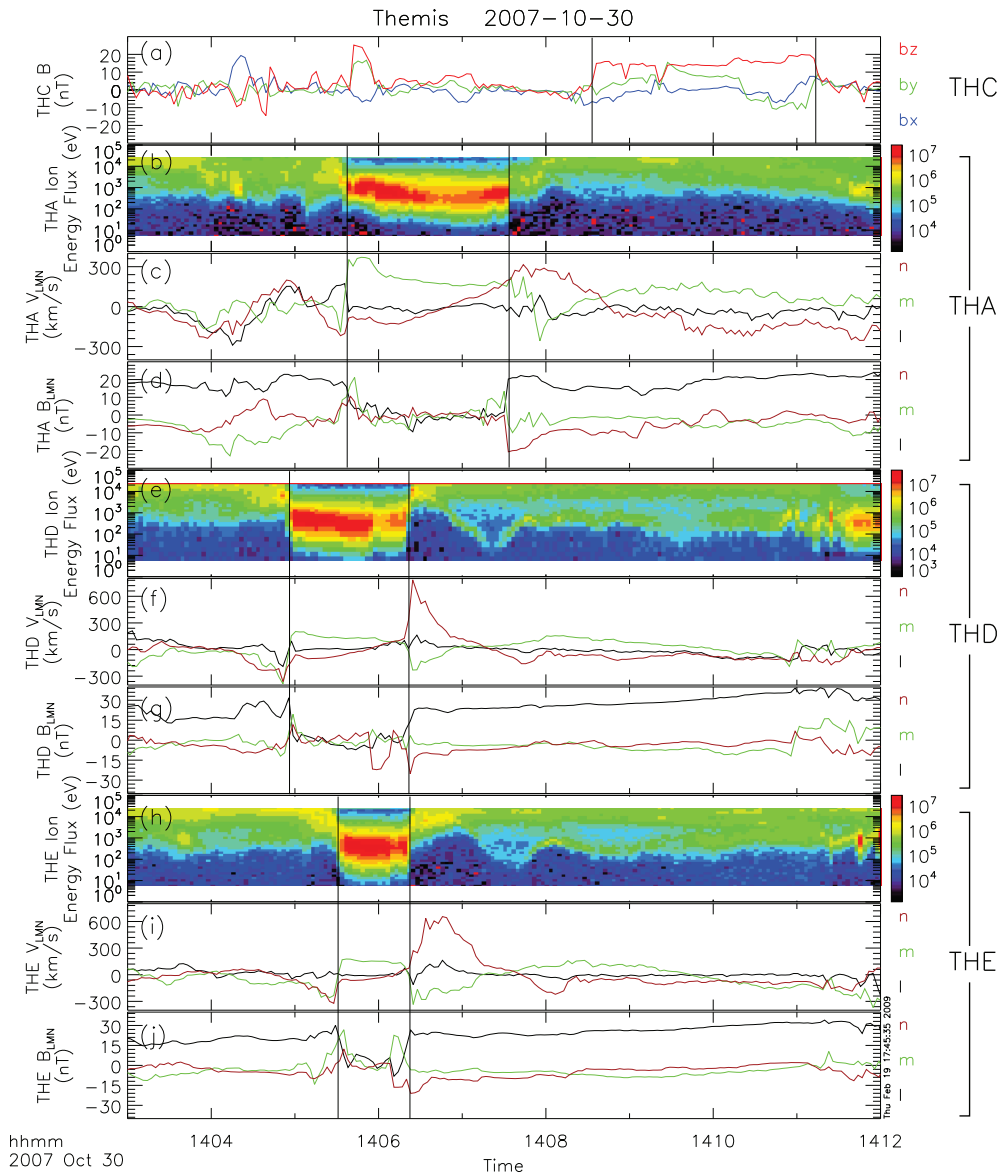
Figure 2. THEMIS A, C, D, and E data. (a) THEMIS C magnetic field. (b–d) THEMIS A ion energy flux spectrogram, velocity, and magnetic field. (e–g) Same for THEMIS D. (h–j) Same for THEMIS E. The velocity and magnetic field for THEMIS A, D, and E are plotted in the LMN coordinate system, using the average magnetopause normal of *Fairfield* [1971], where M is eastward along the model magnetopause, N is normal to the model magnetopause, and L completes the right-handed, orthogonal system. The unit of the spectrograms is eV s^{-1} cm^{-2} sr^{-1} eV^{-1}. The spacecraft are sorted by distance from the model magnetopause, with THEMIS C being in the magnetosheath and the rest being in the magnetosphere. Of the spacecraft in the magnetosphere, THEMIS A is the closest to the model magnetopause. THEMIS A, D, and E have brief encounters with the magnetosheath and THEMIS C encounters the magnetosphere, indicating large-scale magnetopause motion. Magnetopause crossings are indicated by vertical lines.

Spacecraft Used in Calculation	Speed (km/s)
D and E	359
D and A	354
E and A	352

netosheath, and then again as they left the magnetosheath and entered the magnetosphere. For THEMIS C, starting in the magnetosheath, the first crossing was from the magnetosheath to the magnetosphere and the second was from the magnetosphere to the magnetosheath. The shape is drawn to best fit the normals and estimated values. It has been rotated and translated to line up with the different spacecraft while its front end is still attached to the magnetopause. The shape of the magnetopause deformation after the entry of THEMIS C into the magnetosphere is less certain, and has not been drawn. THEMIS C spent 160 s in the magnetosphere, longer than any of the other spacecraft spent in the magnetosheath, which indicates that the outward bulge is larger than the inward bulge.

[22] Just before 1406 UT, THEMIS C had a short encounter with a magnetic field resembling that of the magnetosphere. The timing of the encounter in relation to the timing of magnetopause crossings by the other spacecraft, and the normal vectors resulting from MVA performed on the magnetic field data, was analyzed. For this to be an actual magnetosphere encounter would require a very unusual magnetopause structure and a magnetopause motion at a speed of several thousand km/s. The observed location and timing of the crossings, and the corresponding crossing normals, are better explained by a crossing of the earthward side of a detached flux rope moving antisunward. Unfortunately, there are no particle data from THEMIS C at this time, and the magnetic field data are limited to spin resolution. This makes it difficult to have a positive identification either way.

4.2. Ground Observations

[23] A large, transient magnetopause deformation should have ground signatures. Specifically, one should expect two or more convection vortices to travel from the dayside to the nightside [*Sibeck et al.*, 2003; *Kataoka et al.*, 2004]. A compression followed by an expansion of the magnetosphere is expected to produce a clockwise vortex followed by a counterclockwise vortex.

[24] Figure 3 shows two subsequent SuperDARN [*Greenwald et al.*, 1995; *Chisham et al.*, 2007] convection maps taken at 1406 UT and 1408 UT. In the first we see a counterclockwise vortex, and in the second a clockwise vortex. Although there is some lack of backscatter to constrain the map-potential algorithm, especially on the equatorward edge of the flow vortex at 1406 UT, the observation of these flow vortices in conjunction with the HFA observed by THEMIS B is remarkable. The SuperDARN data do not in actuality show the speed and direction in which the vortices were traveling, as each vortex was detected in only one convection map.

[25] In data from the THEMIS magnetometer array [*Russell et al.*, 2008; *Mende et al.*, 2008; *Glassmeier et al.*, 2008], shown in Figure 4, a magnetic impulse event (MIE) is seen by several magnetometers. The main characteristic of the MIE is a positive peak in the X component,
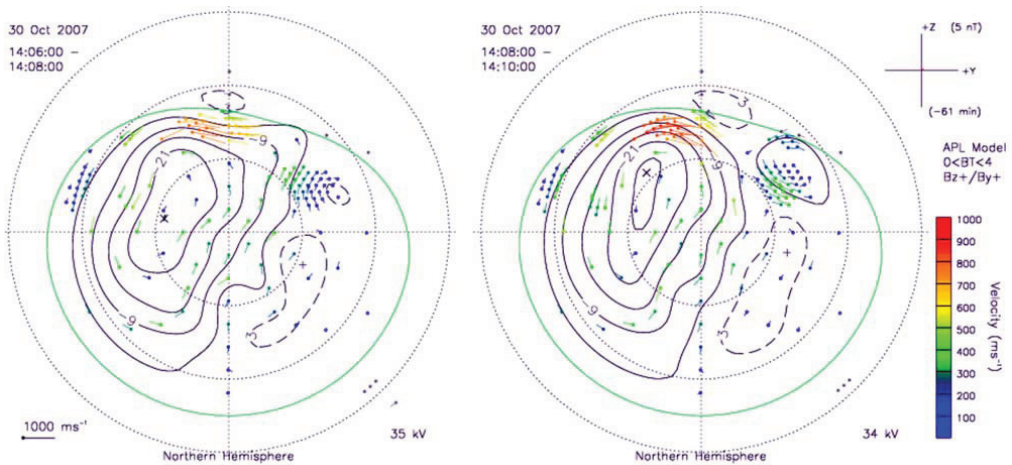

Figure 3. Data from the SuperDARN radar network. Measurements are indicated by dots, with lines pointing out in the direction of the plasma flow. The magnitude of the velocity is indicated by both the length of the line and its color. In areas with no measurements available, the dots and lines are based on a computer model. The black lines are equipotential contours calculated by a computer model, with the cross and plus symbols marking the minimum and maximum values. The green line characterizes the size of the convection zone. SuperDARN observed first a counterclockwise convection vortex, shown on the left, and then a clockwise convection vortex, shown on the right.
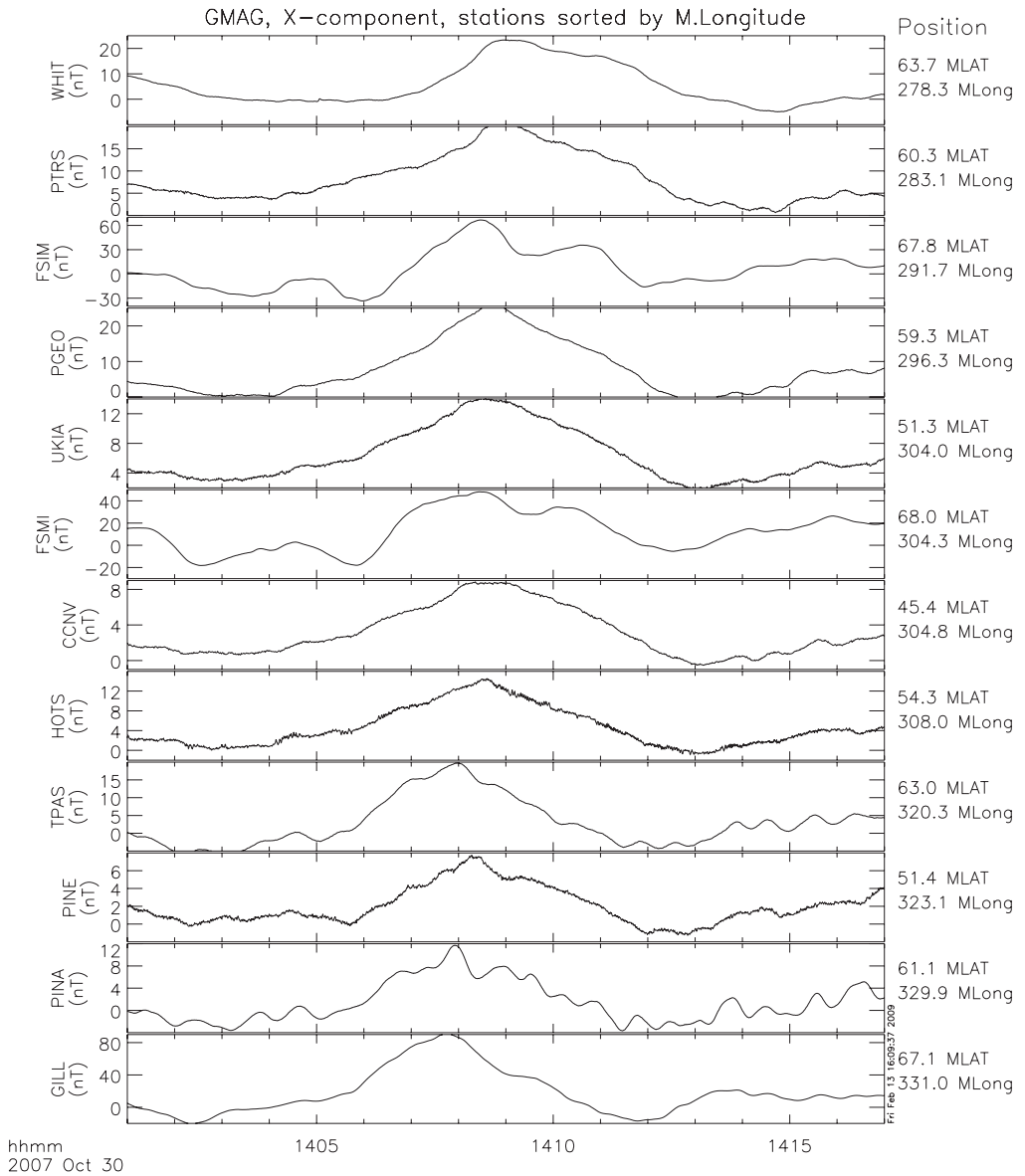
Figure 4. THEMIS ground magnetometer data. Stations are sorted by magnetic longitude from low to high. For each station, the X (north-south) component of the magnetic field is plotted. The long-term average magnetic field has been subtracted. To the right of the plot the positions of the stations in magnetic latitude and longitude are shown. A MIE in the form of a positive peak in the X component is seen moving westward.

which is consistent with a clockwise vortex passing somewhere to the north of the stations. The first station to detect the MIE is GILL, located at 0730 MLT. The central peak of the MIE is seen by GILL at 1407:45 UT, and moves to earlier magnetic local times. WHIT, at 0400 MLT, sees the peak at 1409:05 UT. The ground speed of the MIE is ~25 km/s, going west. The direction is what we expect for a MIE caused by a tailward moving magnetopause deformation at
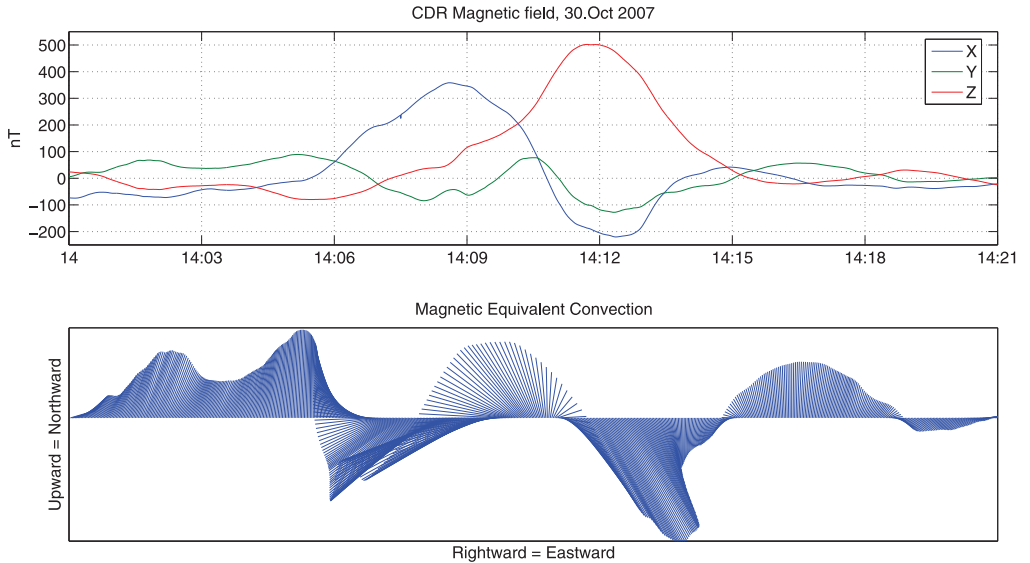
Figure 5. Data from the ground magnetometer station CDR of the MACCS array. (top) Magnetic field disturbance in local geomagnetic coordinates. (bottom) Magnetic equivalent convection (MEC). During the large fluctuations from 1406 to 1415, the MEC is consistent with the passage of a pair of convection vortices.

the dawn flank. We also note that the peak-to-peak amplitude of the MIE tends to be larger at higher latitudes, which is consistent with the convection vortex traveling at a higher latitude than these magnetometers.

[26] At 1408 UT the magnetometer station at Cape Dorset, which is part of the MACCS array [*Hughes and Engebretson*, 1997], was located at 0913 MLT and 73.5 Magnetic latitude, which is very close to the path we expect the vortices to travel. Figure 5 shows data from this station. Between 1406 and 1415 UT, a large magnetic field perturbation is seen, with peak-to-peak amplitudes of 200 nT for By and more than 500 nT for Bx and Bz. Figure 5 (bottom) shows the Magnetic Equivalent Convection (MEC). MEC can be used as an approximation to the plasma convection when the magnetic disturbance is caused mainly by iono-spheric Hall currents. Assuming this to be the case for the interval 1406 to 1415, we see signatures consistent with a counterclockwise vortex followed by a clockwise vortex passing westward, with the vortex centers at a latitude south of the station.

[27] Although convection vortices were observed around the same time as the magnetopause deformations, and moving in the expected way, they were not ordered as expected. Either the compression did not cause a vortex, the ground instrumentation missed a vortex, or our understanding is incomplete. In any case, this shows that the HFA ultimately led to disturbances in the ionosphere.

4.3. ACE and THEMIS B Observations in the Solar Wind

[28] To investigate the cause for the large amplitude perturbation on the magnetopause we examine the upstream solar wind measurements. During this event, the Advanced Composition Explorer (ACE) was at L1 in the pristine solar wind while THEMIS B was in the solar wind just upstream of the dawn bow shock (Figure 1). There were no changes in the solar wind plasma parameters (Figures 6f–6l) measured by ACE that could account for rapid motion of the magnetopause.

[29] Figure 6 shows data from ACE and THEMIS B. Comparing the magnetic field of ACE, located far upstream, to the magnetic field of THEMIS B, located just upstream of the dawn bow shock, we find the drop in B_Z, which is much sharper now, at 1404:40 UT. Following this drop, a small population of high-energy ions is detected. These are ions reflected from the bow shock, to which THEMIS B is now magnetically connected.

[30] At 1406:40 UT, THEMIS B detected something which was not present in the ACE data; an interval of disturbed magnetic field with enhanced ion energy flux between 2–10 keV. There was a flow deflection of many tens of km/s, a drop in the density and a temperature increase, resulting in a drop of the dynamic pressure. These are characteristics of a hot flow anomaly (HFA) [*Schwartz et al.*, 1985; *Thomsen et al.*, 1986].

[31] At this time there was also a change in the magnetic field orientation. The reason that this change caused a HFA, while the much larger change in Bz at 1404:40 UT did not, is the criterion for a HFA that the motional electric field must point toward the discontinuity on at least one side [*Thomsen et al.*, 1993]. Using MVA, the normal to the first discontinuity plane is $(0.91, 0.39, 0.18)_{GSM}$, with an eigenvalue ratio of 7.5. We calculate the convection E field from $\mathbf{E} = -\mathbf{v} \times \mathbf{B}$, and find that the first discontinuity has an
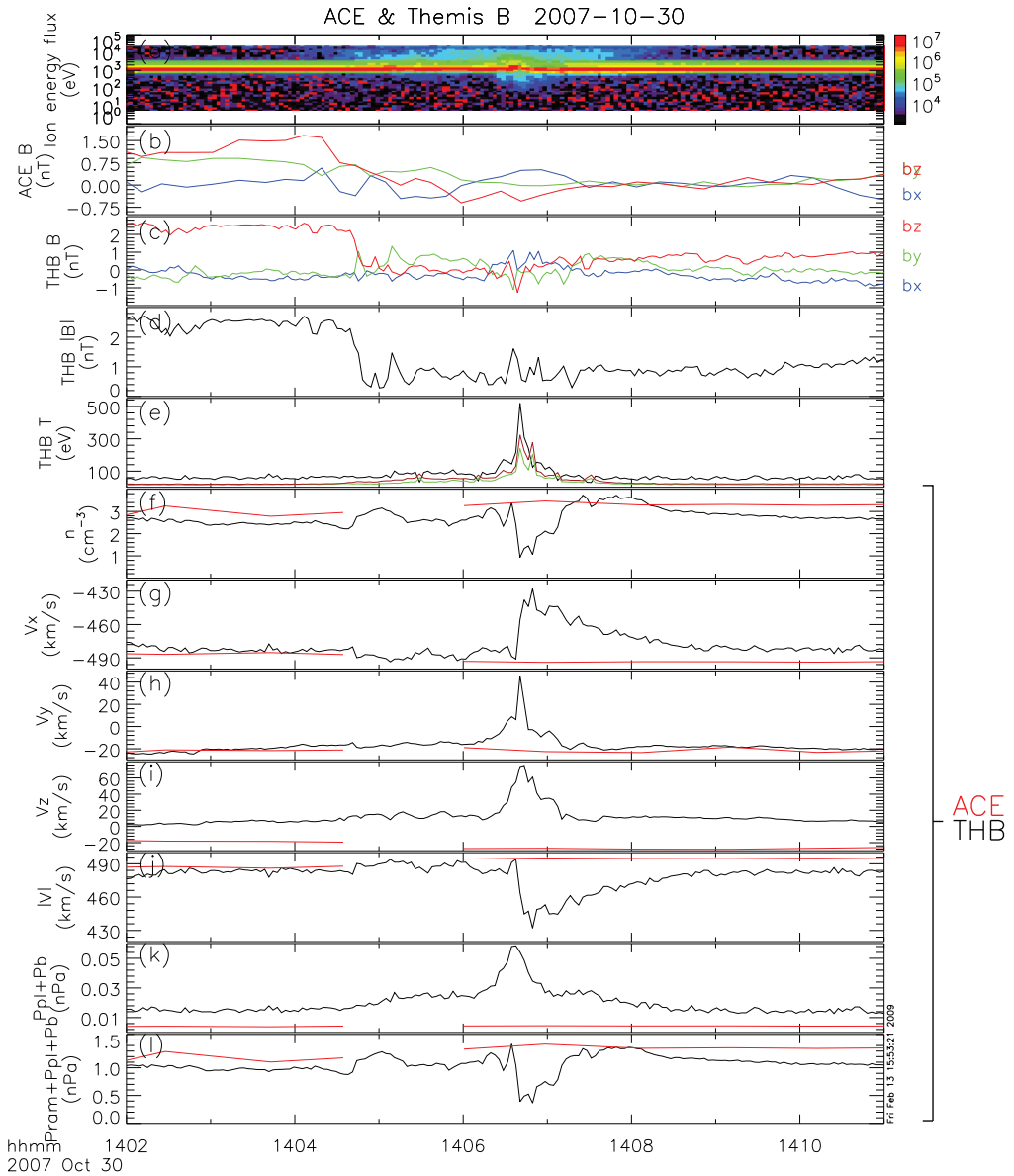
Figure 6. THEMIS B and ACE data. (a) THEMIS B ion energy flux spectrogram (in eV s^{-1} cm^{-2} sr^{-1} eV^{-1}). (b) ACE magnetic field (GSM). (c) THEMIS B magnetic field (GSM). (d) THEMIS B magnetic field magnitude. (e) THEMIS B temperature. (f) Density. (g–j) Velocity GSM X, Y, and Z components and magnitude. (k) Sum of plasma and magnetic pressure. (l) Sum of plasma, magnetic, and ram pressure. In Figures 6f–6l, THEMIS B data are black, and ACE data are red. The ACE data have been time shifted approximately 1 h and 5 min, using first an automatic calculation and then adjusting it according to magnetic signatures close to the time of interest. Around 1406:45, THEMIS B detects magnetic field, density, velocity, and temperature variations consistent with a hot flow anomaly.

electric field pointing away from it on the antisunward side and a very small normal field on the sunward side. The normal to the second discontinuity plane is (0.75, 0.65, −0.10)$_{GSM}$, with an eigenvalue ratio of 3.8. The second discontinuity has a very small normal field on the antisunward side and a field pointing toward it on the sunward side. Thus, only the second discontinuity has an appropriate geometry for HFA formation. The plane of the solar wind discontinuity is shown in Figure 1.

[32] The velocities observed just inside the magnetopause (Figures 2c, 2f, and 2i) are mainly in the N and M directions. This implies that there is no motion of the bulge in the L direction, which points north/south. We interpret this to mean that the bulge is in fact ridge-like, extending north and south. This is consistent with the normal of the discontinuity plane, and the negative M during the outward motion is also consistent with the refilling flow observed in simulation by *Kataoka et al.* [2004].

5. Summary and Conclusions

[33] On 30 October 2007, the five THEMIS spacecraft observed the cause and consequence of extreme motion of the dawn flank magnetopause, with flow speeds in the direction normal to the model magnetopause reaching 800 km/s. Direct observations showed that the magnetopause was displaced outward by at least 4.8 R_E in 59 s. The multispacecraft observations also revealed a bulge on the magnetopause moving tailward at 355 km/s. There was nothing in the solar wind plasma data from ACE that could have caused the magnetopause motion. However, the THEMIS B spacecraft observed the signatures of a hot flow anomaly in the solar wind just upstream of the dawn bow shock, which is likely to be the cause of the fast magnetopause motion.

[34] The following is a summary of our interpretation of the data. On 30 October 2007 a discontinuity in the solar wind magnetic field hit the bow shock. The motional electric field pointed toward the discontinuity on one side, fulfilling an important criterion for HFA generation. The discontinuity swept tailward over the bow shock, with an orientation suited for producing a HFA at the dawn side of the magnetosphere, and THEMIS B did observe signs of a HFA. In the magnetosheath, the HFA created a region of low dynamic pressure surrounded by regions of higher dynamic pressure. As these regions reached the magnetopause, it moved in response to the dynamic pressure variations. As the intersection of the discontinuity with the bow shock moved tailward, so did the HFA structure. The resulting motion of the magnetopause is tailward moving bulges, first inward, then outward. The inward bulge passed over THEMIS A, D and E, allowing us to do a rough reconstruction of its shape. Then, the outward bulge passed THEMIS C, providing direct evidence of rapid, large-amplitude magnetopause motion. The transient deformations of the magnetopause cause field-aligned currents, creating traveling convection vortices which are detected by ground magnetometers.

[35] The multiple spacecraft of the THEMIS mission are clearly a great advantage in the study of events such as these, providing simultaneous measurements from different regions and allowing us to deduce the motion and size of the structures encountered. Our results show that a HFA can have a significant effect on the magnetopause, even when the upstream pristine solar wind was rather unremarkable. This implies that kinetic (non-MHD) effects at the bow shock can have global consequences on the magnetosphere.

[36] We have examined THEMIS data in the period from the start of the mission to June 2008. Though the present event has the highest recorded velocity, there are other events in the THEMIS data set with normal velocities of 400–600 km/s. Further investigation into each event is required to determine if they are also caused by HFAs, and to understand more precisely how the disruption caused by the HFA at the shock is transmitted through the magnetosheath to the magnetosphere.

References

Angelopoulos, V. (2008), The THEMIS mission, *Space Sci. Rev.*, *141*, 5–43, doi:10.1007/s11214-008-9336-1.

Auster, H. U., et al. (2008), The THEMIS fluxgate magnetometer, *Space Sci. Rev.*, *141*, 235–264, doi:10.1007/s11214-008-9365-9.

Berchem, J., and C. T. Russell (1982), The thickness of the magnetopause current layer: ISEE 1 and 2 observations, *J. Geophys. Res.*, *87*, 2108–2114.

Burgess, D. (1989), On the effect of a tangential discontinuity on ions specularly reflected at an oblique shock, *J. Geophys. Res.*, *94*(A1), 472–478.

Burgess, D., and S. Schwartz (1988), Colliding plasma structures: Current sheet and perpendicular shock, *J. Geophys. Res.*, *93*(A10), 11,327–11,340.

Cairns, I. H., D. H. Fairfield, R. R. Anderson, V. E. H. Carlton, K. I. Paularena, and A. J. Lazarus (1995), Unusual locations of Earth's bow shock on September 24–25, 1987: Mach number effects, *J. Geophys. Res.*, *100*, 47–62.

Chisham, G., et al. (2007), A decade of the Super Dual Auroral Radar Network (SuperDARN): Scientific achievements, new techniques and future directions, *Surv. Geophys.*, *28*, 33–109.

Eastwood, J. P., et al. (2008), THEMIS observations of a hot flow anomaly: Solar wind, magnetosheath, and ground-based measurements, *Geophys. Res. Lett.*, *35*, L17S03, doi:10.1029/2008GL033475.

Facsko, G., K. Kecskemety, G. Erdos, M. Tatrallyay, P. W. Daly, and I. Dandouras (2008), A statistical study of hot flow anomalies using Cluster data, *Adv. Space Res.*, *41*(8), 1286–1291, doi:10.1016/j.asr.2008.02.005.

Fairfield, D. H. (1971), Average and unusual locations of the Earth's magnetopause and bow shock, *J. Geophys. Res.*, *76*, 6700–6716.

Farris, M. H., S. M. Petrinec, and C. T. Russell (1991), The thickness of the magnetosheath: Constraints on the polytropic index, *Geophys. Res. Lett.*, *18*, 1821–1824.

Glassmeier, K. H. (1992), Traveling magnetospheric convection twin-vortices—Observations and theory, *Ann. Geophys.*, *10*, 547–565.

Glassmeier, K.-H., et al. (2008), Magnetospheric quasi-static response to the dynamic magnetosheath: A THEMIS case study, *Geophys. Res. Lett.*, *35*, L17S01, doi:10.1029/2008GL033469.

Greenwald, R. A., et al. (1995), DARN/SuperDARN: A global view of the dynamics of high-latitude convection, *Space Sci. Rev.*, *71*, 761–796.

Hughes, W. J., and M. J. Engebretson (1997), MACCS: Magnetometer Array for Cusp and Cleft Studies, in *Satellite-Ground Based Coordination Sourcebook*, Eur. Space Agency Spec. Publ., *ESA SP-1198*, 119–130.

Kataoka, R., H. Fukunishi, L. J. Lanzerotti, T. J. Rosenberg, A. T. Weatherwax, M. J. Engebretson, and J. Watermann (2002), Traveling convection vortices induced by solar wind tangential discontinuities, *J. Geophys. Res.*, *107*(A12), 1455, doi:10.1029/2002JA009459.

Kataoka, R., H. Fukunishi, S. Fujita, T. Tanaka, and M. Itonaga (2004), Transient response of the Earth's magnetosphere to a localized density pulse in the solar wind: Simulation of traveling convection vortices, *J. Geophys. Res.*, *109*, A03204, doi:10.1029/2003JA010287.

Le, G., and C. T. Russell (1994), The thickness and structure of high beta magnetopause current layer, *Geophys. Res. Lett.*, *21*, 2451–2454.

Lin, Y. (2002), Global hybrid simulation of hot flow anomalies near the bow shock and in the magnetosheath, in *Symposium on Intercomparative Magetosheath Studies, Antalya, Turkey, Sep 04–08, 2000, Planet. Space Sci.*, *50*(5–6), 577–591.

McFadden, J. P., C. W. Carlson, D. Larson, M. Ludlam, R. Abiad, B. Elliott, P. Turin, M. Marckwordt, and V. Angelopoulos (2008), The THEMIS ESA Plasma Instrument and in-flight calibration, *Space Sci. Rev.*, *141*, 277–302.

Mende, S. B., S. E. Harris, H. U. Frey, V. Angelopoulos, C. T. Russell, E. Donovan, B. Jackel, M. Greffen, and L. M. Peticolas (2008), The THEMIS array of ground based observatories for the study of auroral substorms, *Space Sci. Rev.*, *141*, 357–387, doi:10.1007/s11214-008-9380.

Paschmann, G., W. Baumjohann, N. Sckopke, T. D. Phan, and H. Lühr (1993), Structure of the dayside magnetopause for low magnetic shear, *J. Geophys. Res.*, *98*, 13,409–13,422.

Phan, T. D., and G. Paschmann (1996), Low-latitude dayside magnetopause and boundary layer for high magnetic shear: 1. Structure and motion, *J. Geophys. Res.*, *101*, 7801–7815.

Russell, C. T., P. J. Chi, D. J. Dearborn, Y. S. Ge, B. Kuo-Tiong, J. D. Means, D. R. Pierce, K. M. Rowe, and R. C. Snare (2008), THEMIS ground-based magnetometers, *Space Sci. Rev.*, *141*, 389–412, doi:10.1007/s11214-008-9337-0.

Schwartz, S. (1995), Hot flow anomalies near the Earth's bow shock, in *Physics of Collisionless Shocks*, edited by C. T. Russell, *Adv. Space Res.*, *15*, 107–116.

Schwartz, S. J., et al. (1985), An active current sheet in the solar wind, *Nature*, *318*, 269–271.

Schwartz, S. J., G. Paschmann, N. Sckopke, T. M. Bauer, M. Dunlop, A. N. Fazakerley, and M. F. Thomsen (2000), Conditions for the formation of hot flow anomalies at Earth's bow shock, *J. Geophys. Res.*, *105*, 12,639–12,650.

Shue, J.-H., J. K. Chao, H. C. Fu, C. T. Russell, P. Song, K. K. Khurana, and H. J. Singer (1997), A new functional form to study the solar wind control of the magnetopause size and shape, *J. Geophys. Res.*, *102*, 9497–9511.

Sibeck, D. G. (1995), The magnetospheric response to foreshock pressure pulses, in *Physics of the Magnetopause*, *Geophys. Monogr. Ser.*, vol. 90, edited by P. Song, B. U. O. Sonnerup, and M. F. Thomsen, pp. 293–302, AGU, Washington, D. C.

Sibeck, D., N. Borodkova, G. Zastenker, S. Romanov, and J. Sauvaud (1998), Gross deformation of the dayside magnetopause, *Geophys. Res. Lett.*, *25*(4), 453–456.

Sibeck, D. G., et al. (1999), Comprehensive study of the magnetospheric response to a hot flow anomaly, *J. Geophy. Res.*, *104*, 4577–4593.

Sibeck, D. G., et al. (2000), Magnetopause motion driven by interplanetary magnetic field variations, *J. Geophys. Res.*, *105*, 25,155–25,169.

Sibeck, D. G., N. B. Trivedi, E. Zesta, R. B. Decker, H. J. Singer, A. Szabo, H. Tachihara, and J. Watermann (2003), Pressure-pulse interaction with the magnetosphere and ionosphere, *J. Geophys. Res.*, *108*(A2), 1095, doi:10.1029/2002JA009675.

Sonnerup, B. U., and L. J. Cahill (1967), Magnetopause structure and attitude from Explorer 12 observations, *J. Geophys. Res.*, *72*, 171–183.

Thomsen, M. F., J. T. Gosling, S. A. Fuselier, S. J. Bame, and C. T. Russell (1986), Hot, diamagnetic cavities upstream from the Earth's bow shock, *J. Geophys. Res.*, *91*, 2961–2973.

Thomsen, M. F., V. A. Thomas, D. Winske, J. T. Gosling, M. H. Farris, and C. T. Russell (1993), Observational test of hot flow anomaly formation by the interaction of a magnetic discontinuity with the bow shock, *J. Geophys. Res.*, *98*, 15,319–15,330.

Winterhalter, D., M. G. Kivelson, C. T. Russell, and E. J. Smith (1981), ISEE-1, -2 and -3 observation of the interaction between an interplanetary shock and the Earth's magnetosphere: A rapid traversal of the magnetopause, *Geophys. Res. Lett.*, *8*, 911–914.

————————————

V. Angelopoulos, IGPP, ESS, University of California, Box 951567, Los Angeles, CA 90095, USA.

J. P. Eastwood, D. Larson, J. P. McFadden, and T. D. Phan, Space Sciences Laboratory, University of California, 7 Gauss Way, Berkeley, CA 94720-7450, USA.

M. J. Engebretson, Department of Physics, Augsburg College, Minneapolis, Minnesota, USA.

K.-H. Fornaçon, IGEP, Technische Universität Braunschweig, D-38106 Braunschweig, Germany.

K. S. Jacobsen and J. I. Moen, Department of Physics, University of Oslo, Postbox 1048, Blindern, N-0316 Oslo, Norway. (knutsj@fys.uio.no)

G. Provan, Department of Physics and Astronomy, University of Leicester, University Road, Leicester LE1 7RH, UK.

D. G. Sibeck, NASA Goddard Space Flight Center, Code 674, Greenbelt, MD 20771, USA.

II

This article is removed.

III

This article is removed.